(12)

ENVIRONMENTAL FATE STUDIES ON CERTAIN MUNITION WASTEWATER CONSTITUENTS

Phase III, Part i — Model Validation

Final Report

By

RONALD J. SPANGGORD
WILLIAM R. MABEY
THEODORE MILL
TSONG-WEN CHOU
JAMES H. SMITH
SHONH LEE

September 1981

Supported by

U.S. ARMY MEDICAL RESEARCH AND DEVELOPMENT COMMAND
Fort Detrick, Frederick, Maryland 21701

Contract No. DAMD17-78-C-8081

SRI International
333 Ravenswood Avenue
Menlo Park, California 94025

Katheryn F. Kenyon, Contracting Officer Technical Representative
U.S. Army Medical Bioengineering Research and Development Laboratory
Fort Detrick, Frederick, Maryland 21701

SECURITY CLASSIFICATION OF THIS PAGE (When Data Entered)

REPORT DOCUMENTATION PAGE

READ INSTRUCTIONS BEFORE COMPLETING FORM

1. REPORT NUMBER	2. GOVT ACCESSION NO.	3. RECIPIENT'S CATALOG NUMBER
-	AD A129393	

4. TITLE (and Subtitle)
Environmental Fate Studies on Certain Munitir . Wastewater Constituents, Phase III, Part I Model Validatior

5. TYPE OF REPORT & PERIOD COVERED
Final Report-Phase III, Part I
September 80 - September 81

6. PERFORMING ORG. REPORT NUMBER
LSU-7934

7. AUTHOR(s)
R. J. Spanggord, William R. Mabey, Theodore Mill, Tsong-Wen Chou, James H. Smith, Shonh Lee

8. CONTRACT OR GRANT NUMBER(s)
DAMD17-78-C-8081

9. PERFORMING ORGANIZATION NAME AND ADDRESS
SRI International
333 Ravenswood Avenue
Menlo Park, CA 94025

10. PROGRAM ELEMENT, PROJECT, TASK AREA & WORK UNIT NUMBERS
62720A.3E162720A835.AA.034.

11. CONTROLLING OFFICE NAME AND ADDRESS
U.S. Army Medical Bioengineering R&D Laboratory
Environmental Protection Research Division
Fort Detrick, Frederick, Maryland 21701

12. REPORT DATE
September 1981

13. NO. OF PAGES
79

14. MONITORING AGENCY NAME & ADDRESS (If diff. from Controlling Office)
U.S. Army Medical Bioengineering R&D Laboratory
Environmental Protection Research Division
Fort Detrick, Frederick, Maryland 21701

15. SECURITY CLASS. (of this report)
Unclassified

15a. DECLASSIFICATION/DOWNGRADING SCHEDULE

16. DISTRIBUTION STATEMENT (of this report)
Approved for public release; distribution unlimited

17. DISTRIBUTION STATEMENT (of the abstract entered in Block 20, if different from report)

18. SUPPLEMENTARY NOTES

19. KEY WORDS (Continue on reverse side if necessary and identify by block number)
2,4,6-Trinitrotoluene (TNT) Hexahydro-1,3,5-trinitro-1,3,5-triazine (RDX), Environmental fate, Holston River, Psuedo-first-order rate constants, Computer modeling, Fate prediction, Photolysis, Biotransformation, Field sampling.

20. ABSTRACT (Continue on reverse side if necessary and identify by block number)
The objective of this report was to validate the SRI Computer Model for estimating the persistence of TNT and RDX [emanating from the Holston Army Ammunition Plant (HAAP) wastestreams] in the Holston River. A two-dimensional compartmentalized river system was developed that describes the dilution of wastestreams entering the Holston River from which the concentrations of RDX and TNT can be estimated. Rate and equilibrium constants for the environmental transport and transformation processes affecting the persistence of TNT and RDX ——>

DD FORM 1 JAN 73 1473
EDITION OF 1 NOV 65 IS OBSOLETE

SECURITY CLASSIFICATION OF THIS PAGE (When Data Entered)

SECURITY CLASSIFICATION OF THIS PAGE (When Data Entered)

19. KEY WORDS (Continued)

20 ABSTRACT (Continued)

were incorporated into the model and concentration-distance pollutant profiles were simulated. Field study data validated the model for RDX, however, sufficient field data could not be obtained to validate the model for TNT.

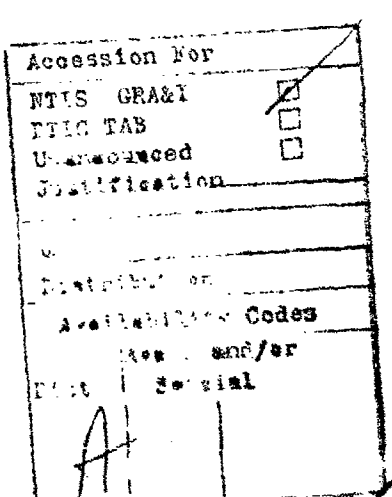

DD FORM 1 JAN 73 1473 (BACK)

EDITION OF 1 NOV 65 IS OBSOLETE

SECURITY CLASSIFICATION OF THIS PAGE (When Data Entered)

EXECUTIVE SUMMARY

Field studies were conducted on the Holston River in the vicinity of Holston Army Ammunition Plant (HAAP) near Kingsport, Tenn. to obtain hydrological and environmental parameters necessary for the computer modeling of the fate (loss and movement) of the munitions-related water pollutants, 2,4,6-trinitrotoluene (TNT) and hexahydro-1,3,5-trinitro-1,3,5-triazine (RDX). Holston River water samples were collected at 0, 4.5, 7.9 and 33.0 km from the discharge point and analyzed for TNT and RDX as a means of validating the concentration-time dependent predictions of the computer model.

A one-dimensional compartmentalized river system was found to accurately predict RDX concentrations at distances greater than 20 km from the discharge point where the HAAP discharge stream becomes uniformly distributed in the Holston River. Up to 20 km, the waste stream is not uniformly distributed and a two-dimensional compartmentalized river system was developed to account for the lateral dispersion effect of HAAP waste streams in the Holston River. The transformation of RDX by environmental processes was determined not to be significant over the studied river reach (33 km), and therefore, the two-dimensional model network describes the dilution processes in the Holston River.

A pseudo-first-order photolysis rate constant of 4.0 day^{-1} and pseudo-first-order biotransformation rate constant of 0.03 day^{-1} for TNT were estimated from laboratory studies and field data. Using the two-dimensional model, concentration-time dependent curves were constructed to predict the concentration of TNT as a function of distance and location (North Bank, Center of River, and South Bank) in the Holston River. Due to the low input of TNT into the Holston River during the field study, sufficient data could not be collected to validate the model for TNT. We were able, however, to determine that the laboratory estimated photo-

chemical rate constant was consistent with that measured in the Holston River.

Field study data collected for the compounds 1-acetyloctahydro-3,5,7-trinitro-1,3,5,7-tetrazocine (SEX), 1-acetylhexahydro-3,5-dinitro-1,3,5-triazine (TAX), and octahydro-1,3,5,7-tetranitro-1,3,5,7-tetrazocine (HMX), suggest that these munitions-related water pollutants do not transform readily in the Holston River.

FOREWORD

We greatfully appreciate the help of the personnel from the U.S. Geological Survey in Knoxville, Tennessee for the collection of Holston River water samples, sediment samples, and turbidity measurements. We also thank our technical staff, Philip Alferness (analytical chemistry), Daniel Haynes (physical transport), Doris Tse (photochemistry), Ellen Shimakawa (biotransformation) for their excellent performance and Leslie Waller, for the final preparation of this report.

TABLE OF CONTENTS

TABLES

FIGURES

I INTRODUCTION

The U.S. Army is in the process of assessing the hazards associated with munitions-related water pollutants in the aquatic environment. Part of this assessment is developing an understanding of the loss and movement (fate) of pollutants when acted upon by various environmental processes. In Phase II of our environmental fate assessment program (Spanggord et al., 1980b), we identified the dominant transport and transformation processes affecting the persistence of 2,4,6-trinitrotoluene (TNT), hexahydro-1,3,5-trinitro-1,3,5-triazine (RDX), 2,4-dinitrotoluene, and trinitroglycerin in the aquatic environment. We also applied the SRI aquatic computer model to selected water bodies receiving munition wastes to generate concentrations of pollutants as a function of time, which would allow the estimation of pollutant concentrations at various locations downstream from the discharge point into these water bodies.

The SRI International aquatic fate model can be used to estimate pollutant concentrations reaching downstream water intake supplies, to estimate exposure levels to various aquatic and mammalian populations, and to estimate pollutant concentrations at plant boundaries in the event that regulatory agencies establish guidelines for the pollutants being discharged. Because of these potential uses, it becomes important to establish the reliability of the model to predict pollutant concentrations under a given set of environmental conditions.

The objective of this study was to validate the SRI computer model used in Phase II by selecting a water body receiving munitions wastes, determine the various environmental input parameters from field measurements, predict pollutant concentrations at selected locations in the water body, and compare the predicted values with actual values obtained during the field study. The chemicals selected for investigation were TNT and RDX.

The results of this study can be used to establish the degree of confidence in the SRI or similar EXAMS model for estimating pollutant concentrations and the extent to which these models may contribute to the overall hazard assessment of munition-related water pollutants.

II BACKGROUND

A. SRI International Model

The study reported herein is based on the application of the SRI International Computer Model (hereafter called the SRI model) to estimate the concentration of pollutants in the Holston River emanating from the Holston Army Ammunition Plant (HAAP) near Kingsport, Tennessee.

The basic model was developed under contract with the U.S. Environmental Protection Agency (Smith et al., 1977) and was applied to the Holston River with some modifications. The model requires information on the hydrologic parameters of the site under investigation and the rate and equilibrium constants for the major transport and transformation processes that act on the chemicals of interest. The hydrologic parameters are determined from field study measurements, and the rate constants are obtained from laboratory studies using the natural water from the site.

The simplest form of the SRI model used to describe a flowing river is the one-dimensional compartmentalized river system. A diagram of this version of the model is shown in Figure 1. In this case, a section of the river is described as one compartment with fixed dimensions of length, width, and depth. This compartment (water compartment) interacts with one sediment compartment directly below it. The chemical disappears at an overall rate controlled by the major kinetic and equilibrium processes established for a specific water body. A river simulation is constructed by joining compartments together, and the loss of chemical in each compartment is determined by the length of time the chemical resides in the compartment and the rate constant for the dominant fate processes. The residence time is calculated from the river flow velocity. Therefore, the input parameters that are required to operate the model, once the rate and equilibrium constants have been measured, include length, width, and depth of the compartment, river flow velocity, initial chemical loading, and parameters that are unique to specific transformation or transport processes such as light intensity (photolysis and oxidation), microbial population (biotransformation), pH (hydrolysis), and wind speed (volatilization).

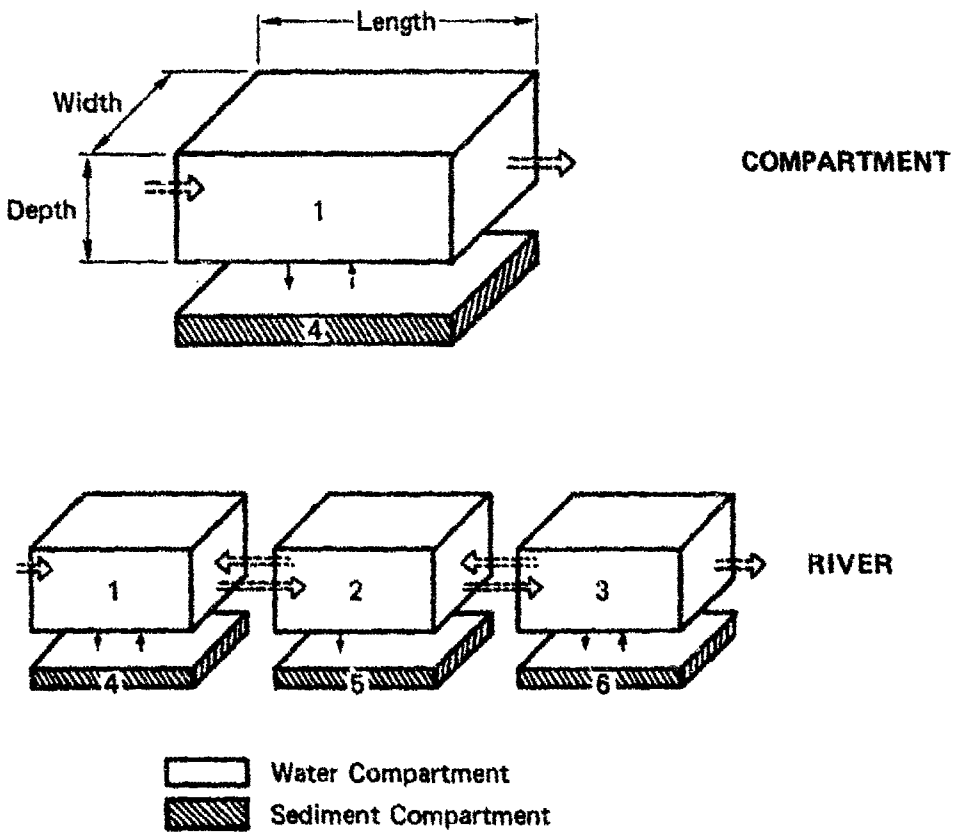

FIGURE 1 PHYSICAL CONFIGURATIONS OF THE COMPARTMENT AND COMPARTMENTALIZED RIVER SIMULATIONS

One of the major assumptions of this model is that each compartment is a completely mixed reactor. To account for cases in which the distribution of a chemical across the river is not uniform, we employed a two-dimensional compartmentalized river system in which lateral flow velocities describe the movement of the chemical across the width of the river (Figure 2). In this case, two or more compartments are formed across the river width. The movement of water from compartment 1 to compartment 2 is equal to the movement of water from compartment 2 to compartment 1. Lateral flows between compartments 2 and 3 are described similarly. Therefore, compartments bordering the discharge bank will dilute continually until homogeneity is achieved across the river. When homogeneity is observed, through either dye studies or the monitoring of persistent chemicals in the river, then the lateral flow velocity may be calculated from distance and river flow velocity measurements.

B. Mathematical Description of Fate Processes

Based on our Phase II studies (Spanggord et al., 1980b), the processes that should be considered to describe the loss of TNT and RDX are photolysis, biotransformation, and sorption.

1. Photochemical Rate Constant

Photolysis can be described by a first order rate expression (Equation 1)

$$\frac{-d[C]}{dt} = k_p[C] \qquad (1)$$

where the rate of loss of chemical, C, is equal to a pseudo-first-order rate constant, k_p, times the chemical concentration, [C].

The rate constant is a function of the sunlight intensity, which varies with the time of day, season, latitude, weather conditions, and the light scattering properties of the water body. To account for the variations in k_p, the rate constant measured in the laboratory (sunlight)

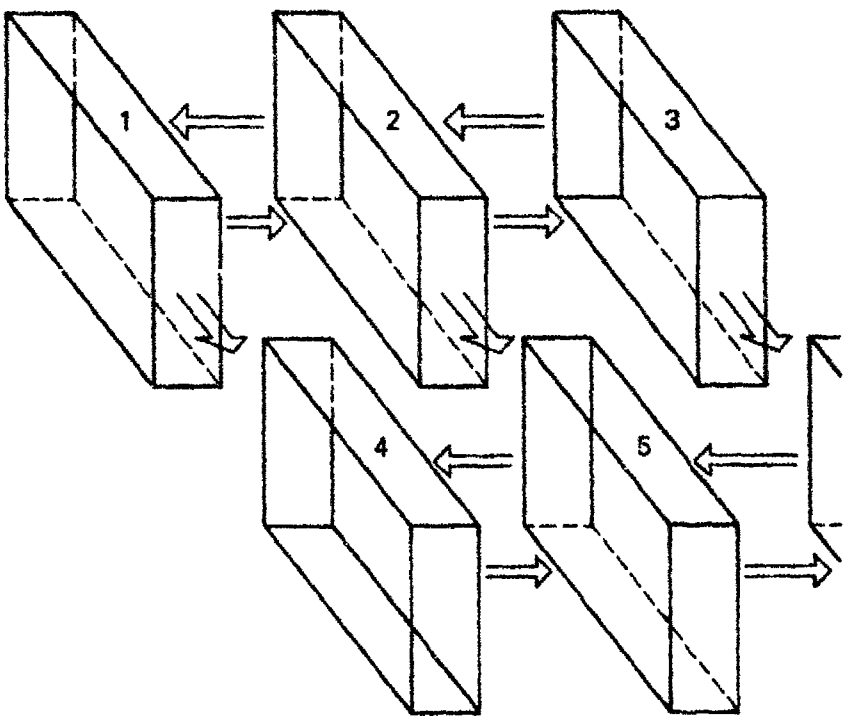

FIGURE 2 PHYSICAL CONFIGURATION OF A TWO-DIMENSIONAL RIVER SIMULATION

at a particular time of day was recalculated by a model program (PHOTO) using Equation 2

$$k_p = k'_p \frac{\sin\left[\frac{3\pi}{2}(t-6)\frac{\pi}{6}\right] + 1.0}{2} \qquad (2)$$

where k'_p is the photolysis rate constant at noon, and t is the time of day. This equation assumes a 12-hour sunlight day starting at 6 AM and ending at 6 PM; k_p reaches a maximum at 12 noon and is zero between 6 PM and 6 AM. A plot of k_p versus time of day appears in Figure 3.

2. Biotransformation Rate Constant

Biotransformation in a natural water body is believed to occur under conditions involving a large microbial population and a low chemical concentration. Under these conditions, the rate of loss of chemical can be described by a first-order rate expression (Equation 3).

$$-\frac{dC}{dt} = k'_b [C] \qquad (3)$$

where k'_b is the pseudo-first order rate constant. This constant is dependent on the microbial population. To account for cases in which the microbial population varies, the model employs a second-order rate expression shown in Equation 4.

$$-\frac{dC}{dt} = k_{b2}[X][C] \qquad (4)$$

where k_{b2} is the second-order rate constant and [X] is the microbial population. The k_{b2} value is calculated from k'_b and [X] using Equation 5.

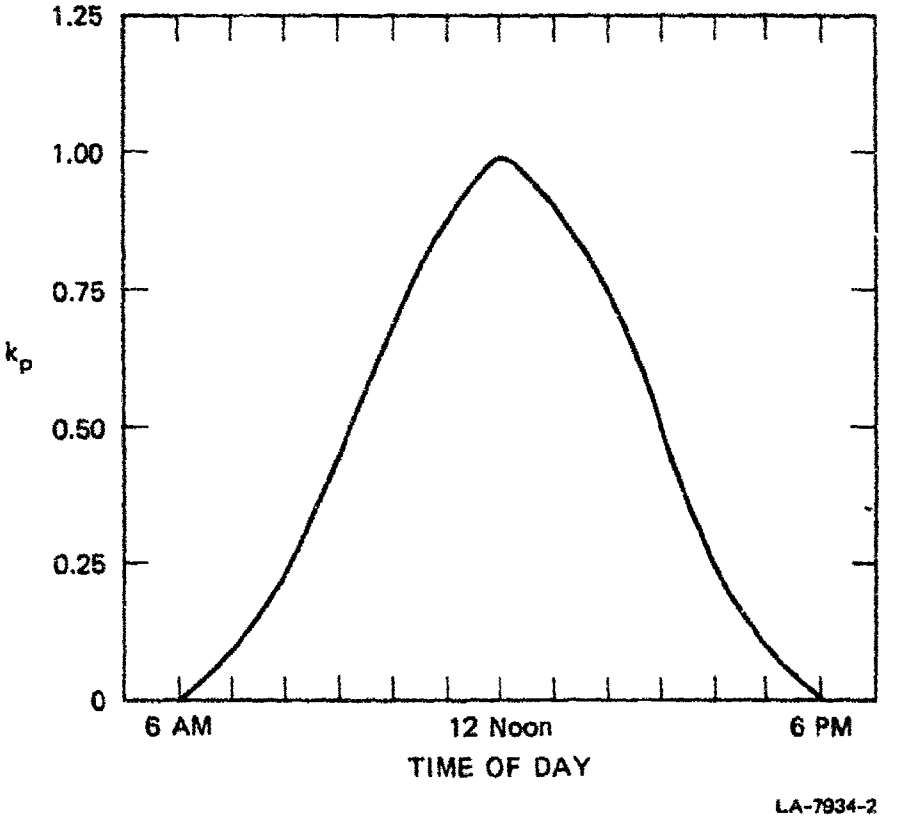

FIGURE 3 PHOTOLYSIS RATE CONSTANT AS A FUNCTION OF TIME OF DAY

$$k_{b2} = k_b' / [X] \quad (5)$$

3. Sediment Sorption Partition Coefficient

The sediment sorption partition constant is obtained from the empirical relationship shown in Equation 6,

$$C_s = k[C_w]^{1/n} \quad (6)$$

where $[C_s]$ is the amount of chemical sorbed per mass of sediment, C_w is the amount of chemical per unit volume of water, and n is a constant. At equilibrium and low chemical concentrations, n is often nearly equal to 1. Under these conditions, the sediment sorption partition coefficient K_s is defined as Equation 7.

$$K_s = \frac{C_s}{C_w} \quad (7)$$

K_s is determined in the laboratory using sediment from the water body under investigation and is applied directly into the model.

C. Model Input-Output Computations

Based on the above discussion, the model input parameters include compartment volume, the photolysis rate constant extrapolated to noon, the second-order biotransformation rate constant and the microbial population, the sediment sorption partition coefficient, and the chemical loading into the first compartment. Sediment settling and scouring rates (calculated from sediment loading data at several locations) are also determined to estimate the fraction of chemical that is not returned to the aqueous phase.

From these data, the model calculates the concentration of chemical transformed and the distribution of chemical between the sediment and aqueous phases. A flow chart of the SRI model for the environmental assessment appears in Figure 4.

The model output consists of changes in chemical concentration and mass in the aqueous and sediment phases of each compartment. Chemical concentration at any point from the discharge point in the water body can then be plotted as a function of time.

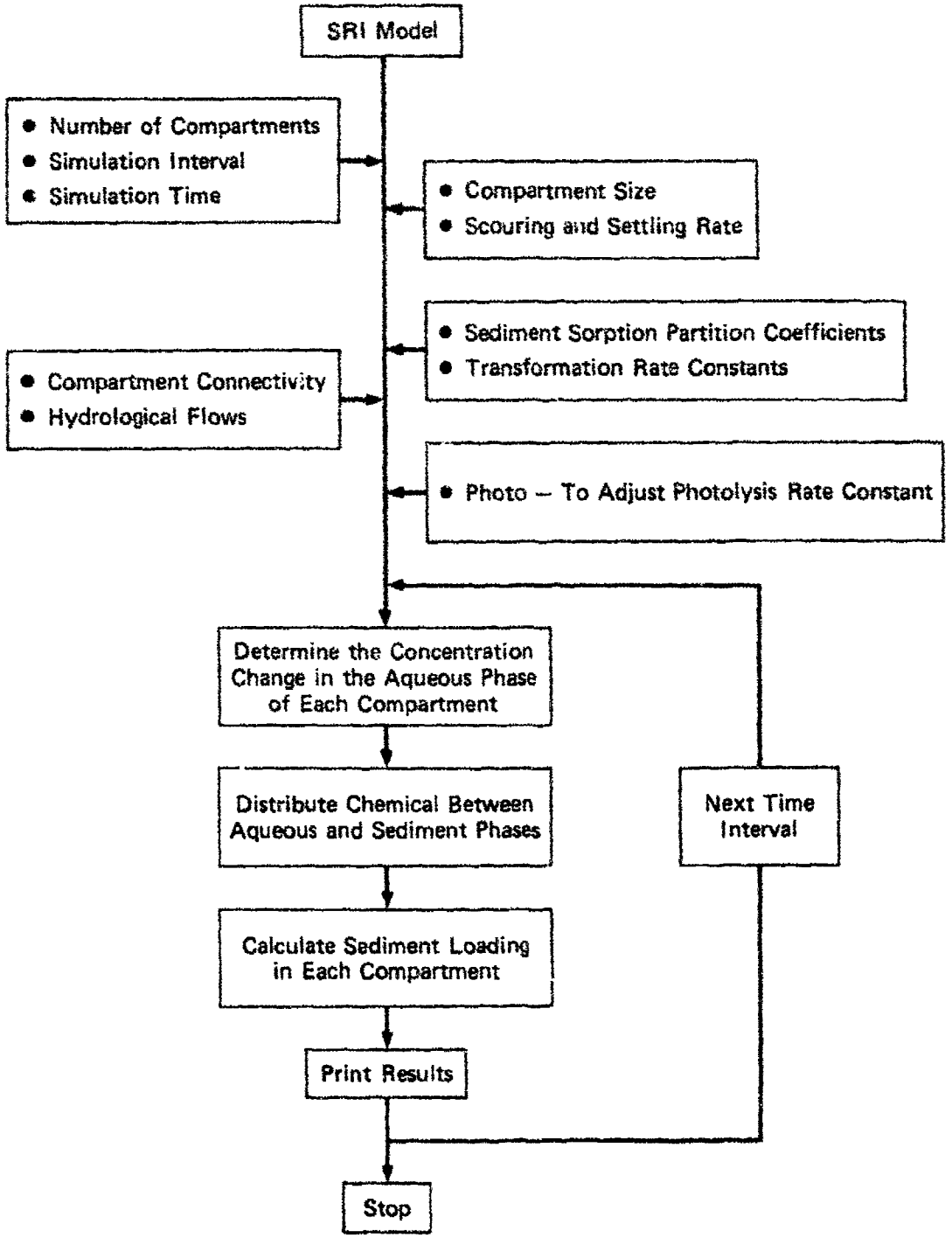

FIGURE 4 FLOW CHART OF THE SRI MODEL FOR ENVIRONMENTAL ASSESSMENT

III METHOD OF APPROACH

A. Site Selection

To validate the SRI model, we chose to study the Holston River, which receives wastes from the Holston Army Ammunition Plant (HAAP) in Kingsport, Tennessee. This river was selected because both TNT and RDX are discharged simultaneously into it, and because we had established the dominant transport and transformation processes for these chemicals in our Phase II laboratory studies. Since RDX was expected not to transform rapidly in the environment, this chemical could serve as a marker compound to estimate the dilution process of waste streams entering the Holston River from HAAP.

A map of the Holston River in the vicinity of the HAAP appears in Figure 5. The major input of TNT and RDX to the Holston River comes from the RDX lines 1-5 at Site A (river mile 139.1, latitude 36° 31'49", longitude 82° 38' 17"). We selected sites 4.5 km (Site B: river mile 136.3, latitude 36° 31' 30", longitude 82° 40' 53"), 7.9 km (Site C: river mile 134.1, latitude 36° 28' 52", longitude 82 41' 02"), and 33.0 km (Site D: river mile 118.5, latitude 36° 28' 08", longitude 82° 51' 00") downstream from Site A as additional sampling points. With these selected sites we expected the TNT concentration to show a significant loss but the RDX concentration to show only a small loss by the time wastewaters discharged at Site A reached Site D. Therefore, by measuring the concentrations of TNT and RDX at these four sites, we could obtain sufficient information for the model validation.

We also measured concentrations of HMX (octahydro-1,3,5,7-tetranitro-1,3,5,7-tetrazocine), SEX (1-acetyloctahydro-3,5,7-trinitro-1,3,5,7-tetrazocine), and TAX (1-acetylhexahydro-3,5-dinitro-1,3,5-triazine), which are discharged from HAAP and also appear at the four collection sites. Although we did not investigate the environmental fate of these compounds, our analytical methodology was developed sufficiently to monitor these compounds along with TNT and RDX. These data may be valuable to the Army when knowledge about the fate of these compounds is desired.

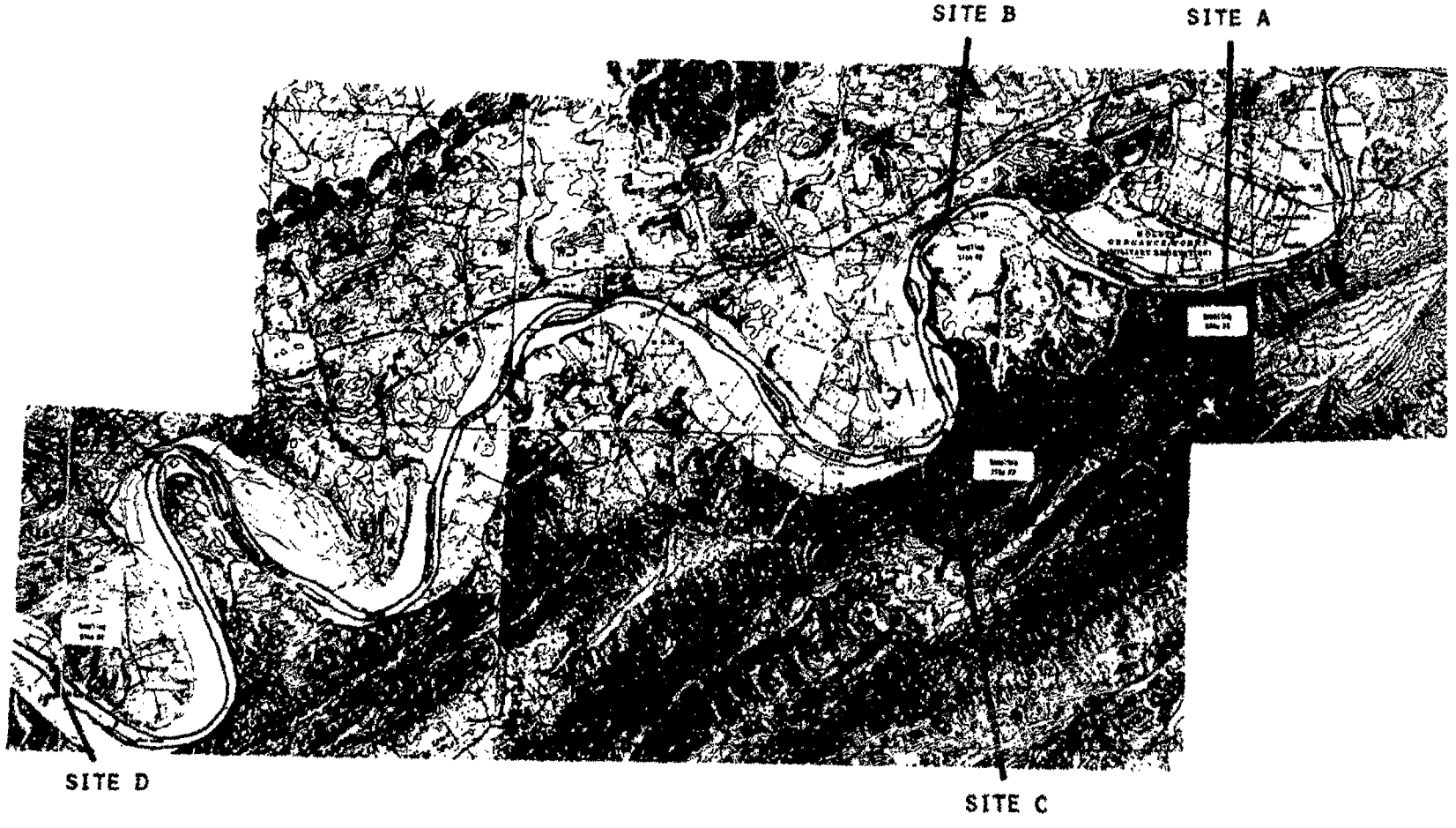

FIGURE 5 MAP OF HOLSTON RIVER IN THE VICINITY OF HOLSTON ARMY AMMUNITION PLANT AND RIVER SAMPLING LOCATIONS

B. Sampling and Hydrologic Data

The collection of water samples and hydrologic data on the Holston River was performed by the U.S. Geological Survey (USGS) under the direction of Dr. Robert Livesey from the Knoxville, Tennessee office. Since the Holston River is approximately 120 meters wide, water samples and hydrologic data were collected from boats. Cables were secured across the river at each sampling site, and markers were placed on the cable approximately 6 meters apart. With the boat attached to the cable at the marker position, the acquisition of samples and data began.

Water samples were collected at each sampling location in amber 1-liter bottles using depth-integrating samplers (Guy and Norman 1970). With this procedure, the water was sampled as an average of the water column at each location. The bottles were labeled and stored in ice until transferred to the laboratory.

Water samples were also collected at every other sampling point for turbidity and suspended sediment analyses. Turbidity analyses were performed by personnel at the University of Tennessee in Knoxville and by personnel at the Holston AAP. Suspended sediment analyses were performed by the USGS in Nashville, Tennessee.

Sediment was collected from the middle of the Holston River at each site along with a water sample for the determination of total microbial counts. Total microbial counts were determined by Ms. Katheryn Kenyon of the U.S. Army Medical Bioengineering Research and Development Laboratory using the serial dilution technique (Bordner and Winter 1979). Sediment samples were analyzed for TNT and RDX by SRI personnel.

At each sampling location, flow velocity and depth measurements were made by USGS personnel according to standard procedures (Buchanan and Somers, 1969). The flow velocity and depth of the RDX lines 1-5 were also determined by USGS personnel. Flow velocity and depth determinations of HMX lines 1-7 and Arnott Creek were estimated by SRI personnel.

C. Determination of TNT, RDX, HMX, SEX, and TAX

The water samples collected from the Holston River were analyzed for TNT, RDX, HMX SEX, and TAX using extraction, concentration, and high-performance liquid chromatographic (HPLC) techniques.

Approximately 1 liter of water collected in an amber bottle with teflon cap was filtered through a 0.45-μ Millipore filter using vacuum filtration. Samples of the filtrate (20-25 ml) were placed in glass vials for analysis by direct aqueous injection into a high-performance liquid chromatograph. The remaining filtrate was measured to the nearest 5.0 ml in a graduated cylinder and added to a 2.0-liter separatory funnel.

The water sample was extracted with 200 ml of dichloromethane (Burdick & Jackson, HPLC grade) with vigorous shaking for 30 seconds. The extract was filtered through 10-15 grams of anhydrous sodium sulfate using vacuum filtration. The extraction of the water was repeated three times with 100-ml portions of dichloromethane.

The dried extracts were combined, transferred to a 1-liter round-bottomed flask, and concentrated to ~ 5 ml using a Buchi rotoevaporator with a water bath temperature of 45°C.

The extracts were transferred to 8-dram glass vials by pipet, the flask rinsed several times with dichloromethane, and the rinses added to the vial. The vials were capped with a Teflon liners, wrapped in aluminum foil, and transported by air with the water samples to SRI for analysis.

The extract was evaporated to dryness using a gentle stream of nitrogen. The residue was dissolved in 0.9 to 1.8 ml of the HPLC mobile phase (65% water, 35% methanol), and an internal standard (3,5-dinitro-toluene) was added. The resulting solution was analyzed by HPLC under the following conditions:

Instrument:	Spectra-Physics Model 3500B Liquid Chromatograph
Column:	Radial Pak A-C_{18} cartridge in a Water's Radial Compression Module
Solvent program:	Methanol/water (35/65) → methanol/water (65/35) in 30 min linear gradient
Flow rate:	1.2 ml/min
Detection:	UV @ 254 nm
Retention Time:	217 s SEX; 277 s TAX; 420 s HMX; 627 s RDX; 1288 s TNT; 1705 3,5-DNT (internal standard)
Injection volume:	100-200 µl

A typical chromatographic profile appears in Figure 6.

The concentration of each component was determined by the internal standard method using peak area measurements determined by a Spectra-Physics "Minigrator" digital integrator. In some extracts, interfering peaks coeluted with the internal standard. In these cases, component concentrations were determined by the external standard method.

The concentration of each component calculated by the peak area determination was then corrected for recovery using precision and accuracy data developed from spiked natural water samples.

Precision and accuracy data were obtained for all six compounds in a natural water (Searsville Pond, Stanford, CA) over three concentration levels including 0.001 $mg\ell^{-1}$, 0.025 $mg\ell^{-1}$, and 1.00 $mg\ell^{-1}$. The percent recovery and the standard deviation (R.S.D.) for each compound at each concentration level appear in Table 1.

The percent recoveries over the three concentration levels were averaged as shown in Table 2 and these recovery factors were applied to the calculation of each munition component. With these values, good agreement was observed between those samples that could be analyzed by direct aqueous injection (no extraction) and the extract of the same sample.

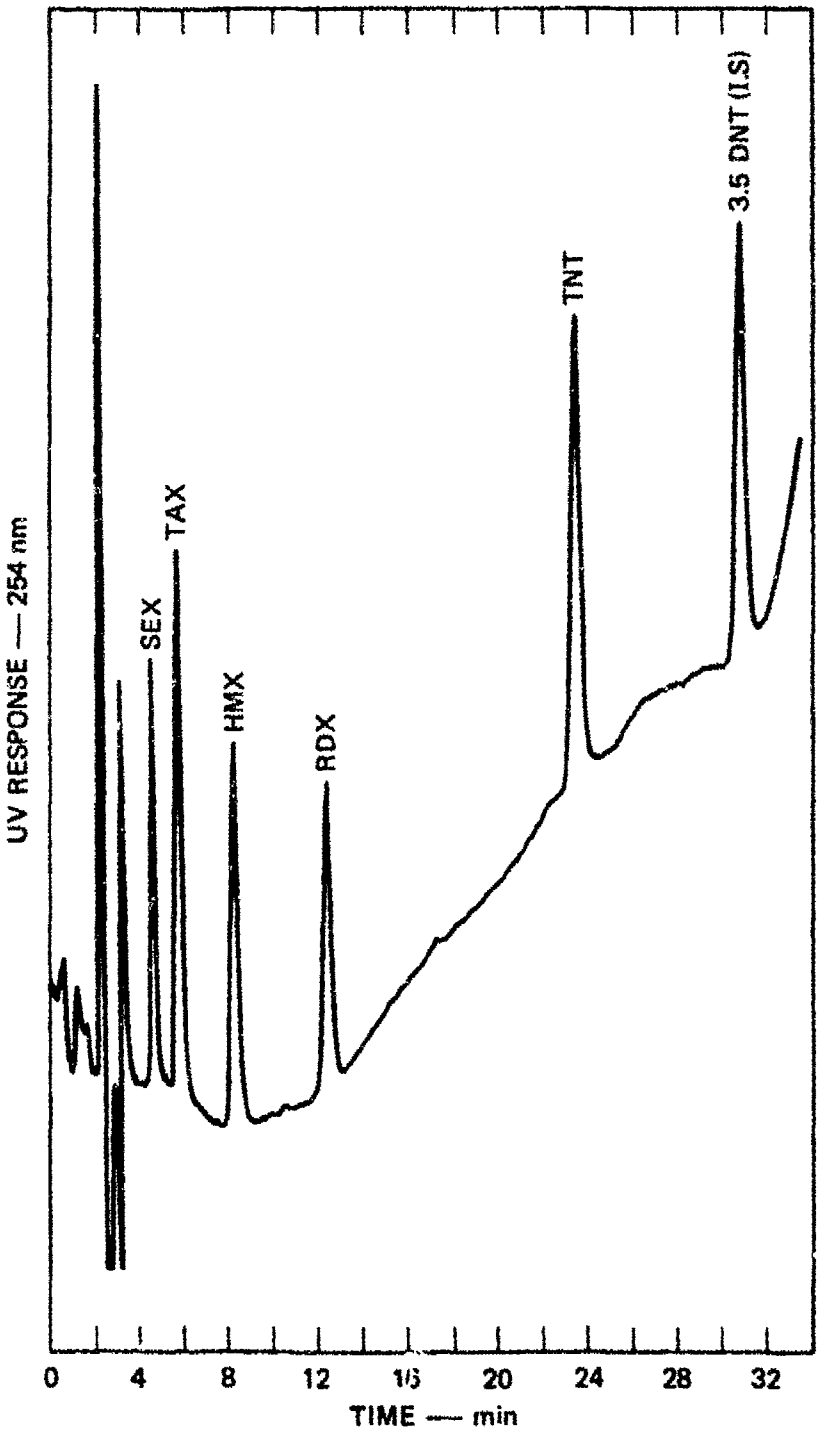

FIGURE 6 HPLC PROFILE OF MUNITIONS COMPONENTS AT 1.0 ppm

Table 1

PERCENT RECOVERY OF MUNITION WASTEWATER CHEMICALS SPIKED INTO NATURAL WATER [a]

	Concentration		
	0.00 mg l^{-1} (N = 4)	0.025 mg l^{-1} (N = 4)	1.00 mg l^{-1} (N = 4)
Compound	Percent Recovery± R.S.D.[b]	Percent Recovery± R.S.D.	Percent Recovery± R.S.D
SEX	52.7 ± 8.2	50.0 ± 11.5	48.5 ± 19.5
TAX	71.9 ± 4.5	67.4 ± 14.1	62.8 ± 6.7
HMX	99.9 ± 2.6	92.6 ± 0.2	90.6 ± 6.4
RDX	96.1 ± 5.2	98.6 ± 8.0	93.9 ± 6.4
TNT	89.9 ± 7.9	91.1 ± 2.9	89.2 ± 10.0

[a] Natural water from Searsville pond, Stanford, CA.
[b] Relative standard deviation.

D. Sediment Analyses

Sediment samples collected in glass jars were allowed to settle, and the aqueous phases were decanted from the jars. An aliquot of the remaining suspension was weighed and dried overnight at 120°C. The before and after drying weights of sediment gave the water content of the sediment. The sediment suspensions could therefore be handled without altering the sediment properties.

A sediment sample was analyzed by stirring approximately 100 g of moist sediment with 100 ml of ethyl acetate in an Erlenmeyer flask for 3 hours. The ethyl acetate was decanted, an additional 50 ml of solvent was added, and the suspension was stirred for 10 minutes. The solvent was decanted, combined with the first extract, and rotary-evaporated to dryness. The residue was dissolved in a few milliliters of methanol. The resulting solution was passed through a C_{18} Sep-Pak as a cleanup step and washed with a small amount of methanol, and the eluent was evaporated to dryness with a gentle stream of nitrogen. The residue was dissolved in a methanol:water mixture (50:50) and analyzed by HPLC as described previously.

E. Confirmatory Analyses

The presence of low levels of TNT, 4-amino-2,6-dinitrotoluene (4-A-2,6-DNT), and 2-amino-4,6-dinitrotoluene (2-A-4,6-DNT) found by HPLC was confirmed by gas chromatographic analysis and mass spectrometric analysis performed under the following conditions.

Instrument:	Varian 3700 Gas Chromatograph
Column:	1.8 m × 2.0 mm glass column packed with 3% SP2100 on 80/100 mesh Chromosorb W-HP
Temperature:	180 (4 min hold) + 230 @ 2° min^{-1}
Flow rate:	25 ml min^{-1} N_2
Detector:	Electron capture (ECD) or an LKB 9000 mass spectrometer

Table 2

AVERAGED PERCENT RECOVERY OF MUNITION WASTEWATER CHEMICALS FROM SPIKED NATURAL WATER[a]

Compound	Percent Recovery ± R.S.D.
SEX	50.4 ± 12.9
TAX	67.3 ± 9.8
HMX	94.2 ± 5.5
RDX	95.9 ± 6.1
TNT	89.9 ± 7.0

[a]Natural water from Searsville pond, Stanford, CA.

Gas chromatography with electron capture detection (GC/ECD) was based on comparative analysis with the retention times of authentic standards. Mass spectrometric identification was based not only on retention time but also on single ion monitoring of major ion fragments (m/e = 210 for TNT; m/e = 180 for 4-A-2,6-DNT and 2-A-4,6-DNT).

Samples were collected from the HPLC according to their elution volume, concentrated to dryness using nitrogen gas, and dissolved in a small amount of methanol before gas chromatographic analysis.

F. Rate and Equilibrium Constants

The photochemical rate constant for TNT was measured in North and South Fork Holston River water obtained upstream from the HAAP discharge lines. TNT was spiked into the water, and photolysis experiments in sunlight were performed under several conditions— in filtered sterilized water in borosilicate tubes and in 10 cm × 200 cm open crystallizing dishes and in unfiltered water containing suspended sediment in open dishes. The TNT concentrations were measured as a function of time, and the rate constant was calculated from the integrated form of Equation 1 shown in Equation 8,

$$\ln \frac{C_o}{C_t} = k_p t \qquad (8)$$

where C_o and C_t are the TNT concentrations at times zero and t. Regression of ln C versus t gives the slope k_p.

Pseudo-first-order rate constants for the photolysis of RDX and the biotransformation of TNT, as well as the TNT and RDX sorption partition coefficients, were obtained from our Phase II report (Spanggord et al., 1980b). A second-order rate constant for the biotransformation of TNT was obtained using Equation 5.

IV RESULTS

The field sampling studies of the Holston River took place on April 22 and 23, 1981. Weather conditions were hazy and sunny on April 22 and rainy on April 23. Rains from earlier in the week in West Virginia created above average flows (runoff) in the North Fork of the Holston River; however, the river receded during the collection of data.

On April 22, the total flow contributions from the North and South Forks of the Holston River were 71.5 m^3s^{-1} and 22.2 m^3s^{-1} respectively. On April 23, flows were 73.5 m^3s^{-1} and 21.6 m^3s^{-1}, respectively. These values were obtained from upstream gaging stations on each fork. Flow measurements downstream at Surgoinsville gaging station (Site D) were 120.8 $m^3\ s^{-1}$ on April 22 and 89.9 $m^3\ s^{-1}$ on April 23.

A. Hydrological Data

1. Streambed Contour and River Flow Velocity

From the depth measurements at each sampling location (Table 3), we constructed a streambed contour for each of the four sites investigated. Contours for sites A, B, C, and D appear in Figure 7. At each section, the cross-sectional area was calculated (distance between sections times depth) and summed across the width of the river to yield a total cross-sectional area. The total cross-sectional area was divided by the total summed flow rate to yield the river flow velocity. These data appear in Table 4. The flow velocity was used to estimate the residence time of the water in each compartment.

The flow rates at sites A, B, and C vary within 4%, which may be due to the natural transportation of water into and out of each site or the accuracy of the measurement. However, a large reduction in total flow was noted between Sites C and D (17%). Seepage may be one factor contributing to the loss of water; however, no causes for this loss were identified.

2. Water Quality Parameters

Water quality parameters including temperature, pH, dissolved oxygen, and conductivity were measured at each sampling station. These data appear in Table 5. These data indicate that the Holston River is in good

Table 3

DEPTH AND FLOW MEASUREMENTS ACROSS THE HOLSTON RIVER AT FOUR SAMPLING LOCATIONS

Site	Section	Station*	Time	Depth (feet)	Flow ($ft^3 s^{-1}$ sec)
A	A- 1	25	9:20	5.7	63.9
	A- 2	40	9:30	6.0	132
	A- 3	55	9:35	6.0	139
	A- 4	70	9:45	5.3	161
	A- 5	90	9:50	6.1	238
	A- 6	110	9:55	5.9	203
	A- 7	130	10:00	6.0	172
	A- 8	150	10:10	5.7	182
	A- 9	170	10:15	5.5	167
	A-10	190	10:20	5.7	173
	A-11	210	10:27	5.5	190
	A-12	230	10:32	5.7	189
	A-13	250	10:45	6.3	214
	A-14	270	10:52	5.7	201
	A-15	290	11:00	5.2	180
	A-16	310	11:05	5.1	199
	A-17	335	11:09	5.6	162
	A-18	360	11:18	5.3	169
	A-19	385	11:25	5.0	140
	A-20	410	11:30	4.5	190
	A-21	450	11:35	4.0	69.6
			Total Flow		3524.5

Table 3 (Continued)

Site B	Section	Station	Time	Depth	Flow
B	B- 1	20	11:15	5.1	31.0
	B- 2	40	11:21	5.7	83.2
	B- 3	60	11:25	6.5	138
	B- 4	80	11:30	6.5	120
	B- 5	95	11:34	6.9	148
	B- 6	110	11:39	7.3	150
	B- 7	125	11:43	7.6	135
	B- 8	135	11:49	7.9	118
	B- 9	145	11:57	8.2	121
	B-10	155	12:01	8.1	117
	B-11	165	12:05	8.4	126
	B-12	175	12:10	8.5	106
	B-13	185	12:15	9.7	133
	B-14	200	12:19	11.1	189
	B-15	210	12:25	11.3	145
	B-16	220	12:21	11.4	150
	B-17	230	12:34	10.6	146
	B-18	240	12:40	10.1	143
	B-19	250	12:43	9.3	126
	B-20	265	12:48	10.4	169
	B-21	275	12:55	11.3	180
	B-22	290	13:01	10.2	177
	B-23	305	13:05	9.9	194
	B-24	325	13:11	9.7	183
	B-25	340	13:16	9.4	83.8
			Total Flow		3412

Table 3 (Continued)

Site C	Section	Station	Time	Depth	Flow
C	C- 1	20	14:35	6.0	185
	C- 2	50	14:38	4.6	251
	C- 3	70	14:45	4.5	197
	C- 4	90	14:50	4.3	198
	C- 5	110	15:00	5.6	246
	C- 6	130	15:03	6.0	239
	C- 7	150	15:06	4.5	179
	C- 8	170	15:12	4.1	141
	C- 9	190	15:18	4.7	176
	C-10	215	15:22	3.7	161
	C-11	240	15:26	5.8	274
	C-12	265	15:30	6.7	242
	C-13	290	15:40	7.3	331
	C-14	315	15:45	3.5	164
	C-15	340	15:50	5.0	225
	C-16	365	15:55	3.8	175
	C-17	390	16.00	3.0	144
	C-18	415	16:05	3.8	135
			Total Flow		3663

Table 3 (Concluded)

Site D	Section	Station	Time	Depth	Flow
D	D- 1	15	9:20	5.5	22.3
	D- 2	30	9:30	5.8	40.0
	D- 3	45	9:40	6.0	63.0
	D- 4	60	9:45	6.6	74.0
	D- 5	72	9:50	6.2	71.4
	D- 6	84	10:00	7.0	76.4
	D- 7	96	10:05	7.1	92.0
	D- 8	108	10:10	7.2	93.3
	D- 9	120	10:15	7.0	105
	D-10	135	10:23	7.8	140
	D-11	150	10:30	7.5	141
	D-12	165	10:40	8.5	177
	D-13	180	10:48	8.2	175
	D-14	195	10:50	9.0	192
	D-15	210	11:00	9.1	186
	D-16	225	11:07	10.6	159
	D-17	240	11:15	11.4	239
	D-18	255	11:22	13.0	261
	D-19	270	11:30	11.0	233
	D-20	285	11:37	10.5	277
	D-21	310	11:45	8.0	224
			Total Flow		3031.4

*Station refers to the distance from the North Bank (feet).

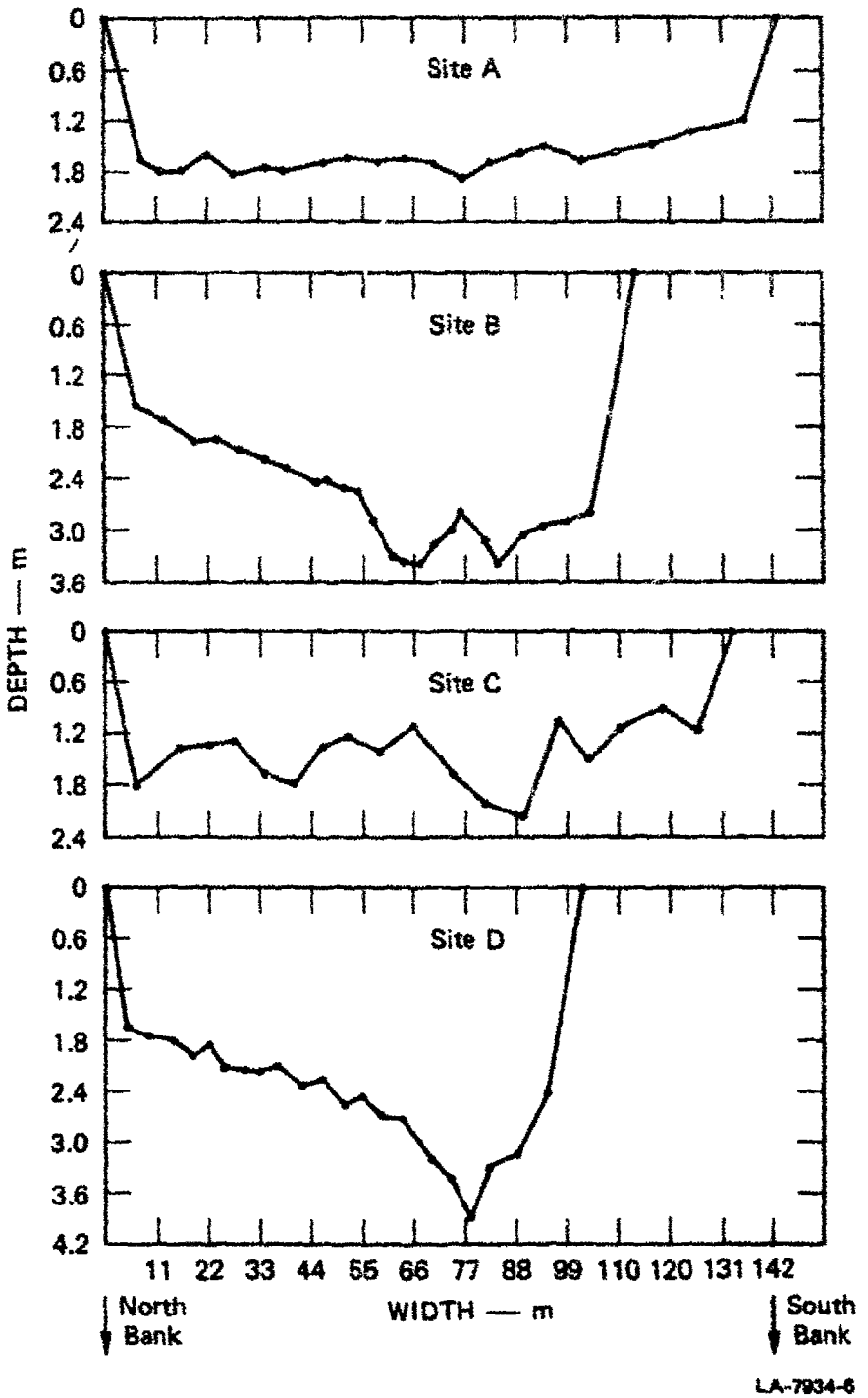

FIGURE 7 STREAMBED CONTOURS OF EACH SAMPLING LOCATION

Table 4

WIDTH, EFFECTIVE DEPTH, TOTAL CROSS SECTIONAL AREA, TOTAL FLOW, AND FLOW VELOCITY FOR EACH SAMPLING SITE

Site	Width		Effective Depth		Total Cross-Sectional Area		Total Flow		Flow Velocity	
	m	(ft)	m	(ft)	m^2	(ft^2)	$m^3\ s^{-1}$	($ft^3\ s^{-1}$)	$m\ s^{-1}$	($ft\ s^{-1}$)
A	138	(457)	1.6	(5.2)	220	(2376)	98	(3534)	0.45	1.5
B	108	(356)	2.5	(8.2)	267	(2919)	95	(3412)	0.36	1.2
C	130	(430)	1.4	(4.6)	182	(1978)	102	(3663)	0.56	1.9
D	102	(335)	2.4	(7.8)	241	(2613)	85	(3041)	0.35	1.2

Table 5

THE TEMPERATURE, pH, DISSOLVED OXYGEN, AND CONDUCTIVITY MEASURED AT EACH SECTION AND SITE

Section	Temperature °C				pH				Dissolved oxygen (ppm)				Conductivity (µmhos)			
	Site				Site				Site				Site			
	A	B	C	D	A	B	C	D	A	B	C	D	A	B	C	D
1	14.2	14.5	16.2	16.5	7.2	7.1	7.2	7.6	9.3	8.5	10.0	6.4	257	229	264	280
2	13.7	14.6	16.1	16.5	7.2	7.1	7.2	7.4	9.6	8.7	10.0	7.6	228	227	266	280
3	13.5	14.6	16.1	16.5	7.2	7.1	7.2	7.6	9.8	8.7	10.0	6.8	223	227	268	265
4	13.5	14.7	16.2	16.6	7.2	7.1	7.3	7.7	9.8	8.8	10.0	6.9	222	228	269	255
5	13.6	14.8	16.2	16.7	7.2	7.1	7.3	7.7	9.8	8.7	10.0	6.8	224	232	270	255
6	13.6	14.8	16.3	16.6	7.3	7.1	7.2	7.7	9.8	8.8	9.8	7.0	226	233	273	280
7	13.7	14.8	16.4	16.6	7.2	7.1	7.2	7.7	9.7	8.7	9.9	7.0	229	236	276	260
8	13.8	15.1	16.4	16.6	7.2	7.1	7.2	7.7	9.6	8.7	9.9	6.9	231	242	279	255
9	13.9	15.2	16.4	16.6	7.2	7.1	7.2	7.7	9.5	8.6	10.0	7.0	239	246	281	280
10	14.1	15.2	16.5	16.6	7.2	7.1	7.2	7.7	9.5	8.6	9.9	7.0	245	251	286	280

Table 5 Continued

THE TEMPERATURE, pH, DISSOLVED OXYGEN, AND CONDUCTIVITY
MEASURED AT EACH SECTION AND SITE

Section	Temperature °C				pH				Dissolved oxygen (ppm)				Conductivity (µmhos)			
	Site				Site				Site				Site			
	A	B	C	D	A	B	C	D	A	B	C	D	A	B	C	D
11	14.2	15.4	16.6	16.6	7.2	7.1	7.1	7.7	9.3	8.6	9.8	7.0	253	255	292	280
12	14.5	15.5	16.7	16.8	7.1	7.1	7.1	7.7	9.2	8.6	9.6	7.0	267	258	295	282
13	14.7	15.5	16.8	16.8	7.1	7.1	7.1	7.7	8.9	8.5	9.6	7.0	279	258	299	280
14	15.0	15.6	16.8	16.8	7.1	7.1	7.1	7.0	8.6	8.5	9.5	7.4	293	262	303	280
15	15.5	15.8	17.1	16.7	7.1	7.1	7.1	6.8	8.3	8.4	9.4	7.4	315	270	307	285
16	15.3	15.4	17.2	16.8	7.0	7.1	7.1	7.4	8.0	8.4	9.2	7.4	328	273	309	285
17	16.3	16.0	17.2	16.8	7.0	7.1	7.1	7.5	7.6	8.4	9.2	6.8	357	277	310	285
18	16.9	16.1	17.3	16.8	7.0	7.1	7.1	7.5	6.9	8.3	9.4	7.0	384	279	305	288
19	17.2	16.2	17.2	16.9	7.0	7.1	7.1	7.5	6.9	8.3	—	7.0	403	289	—	288
20	17.5	16.2	—	17.0	7.0	7.1	—	7.5	6.6	8.3	—	6.8	408	286	—	290
21	17.8	16.3	—	17.0	6.9	7.1	—	7.5	5.7	8.3	—	6.6	408	288	—	263
22	—	16.4	—	—	—	7.1	—	—	—	8.3	—	—	—	291	—	—
23	—	16.4	—	—	—	7.1	—	—	—	8.2	—	—	—	294	—	—
24	—	16.7	—	—	—	7.1	—	—	—	8.1	—	—	—	302	—	—
25	—	16.9	—	—	—	7.0	—	—	—	7.9	—	—	—	308	—	—

ecological condition. Some divergence of the data--such as that on conductivity at Sites A, B, and C--indicates that the river is not well mixed within the boundaries of HAAP.

3. Suspended Sediments and Turbidity

The suspended sediment and turbidity were measured at several stations at each site. These data appear in Table 6. The suspended sediments were found to decrease from approximately 126 mgl^{-1} at Site A to 22 mgl^{-1} at Site D. It is expected that the bottom sediment layer will increase under these conditions. Because both TNT and RDX sorbed to sediment weakly, we expect only small losses of these chemicals from the water to the sediment. Turbidity also decreased from Site A to Site D in a fashion similar to the sedimentation.

4. Microbial Populations

The microbial population was determined from one section at each sampling site. These results appear in Table 7. The values (10^3 to 10^4 cells ml^{-1}) are low compared to the value of 10^6 cells ml^{-1} usually found in a running stream. Higher values were expected because of waste from upstream industries and the high sediment loadings. However, the observed values were used in the model, and therefore biotransformation was expected to contribute little to the overall loss of TNT or RDX.

5. Input Concentrations of Chemicals from HAAP Wastestreams

Three wastestreams provide chemical input into the Holston River from HAAP. These wastestreams are the HMX lines 1-7, RDX lines 1-5, and Arnott Creek. RDX lines 1-5 were believed to be the major input of TNT and RDX. The HMX lines 1-7 enter the Holston River approximately 600 m above the RDX lines, while Arnott Creek enters the Holston River approximately 4 km downstream from the RDX lines. A map designating the input streams is shown in Figure 8.

The RDX input stream travels through an underground culvert and surfaces approximately 15 m from the Holston River, where it mixes with cooling water. The flow of the stream prior to mixing with the cooling water was estimated at 0.07 $m^3\ s^{-1}$ (2.63 cfs).

Table 6
SUSPENDED SEDIMENT AND TURBIDITY MEASUREMENTS
AT SITES A, B, C, AND D

Site	Station 2	4	6	8	10	12	14	16	18	20
	Suspended Sediments (mg ℓ^{-1})									
A	121	126	126	124	116	109	103	75	88	34
B	236	88	99	98	93	90	92	84	81	85
C	67	91	90	94	90	87	37	79	72	-
D	22	29	31	32	35	38	34	44	43	45
	Turbidity (mg ℓ^{-1})									
A	14	12	18	15	12	11	12	8	6	3
B	21	17	18	23	26	21	21	22	21	23
C	10	11	12	11	12	12	11	8	8	-
D	2	3	3	4	4	2	4	4	4	4

Table 7

MICROBIAL POPULATIONS MEASURED IN THE HOLSTON RIVER AT EACH SAMPLING SITE

Sample	Dilution	Raw Counts[a]	Avg ml^{-1}[b]	CFU ml^{-1}[c]
A-7	10^{0}	228, 253, 265	2487	---
	10^{-1}	63, 98, 39	667	---
	10^{-2}	5, 6, 2	43	4.5×10^{3}
	10^{-3}	0, 0, 0	---	---
	10^{-4}	0, 0, 0	---	---
B-13	10^{-0}	TNTC x 3	---	---
	10^{-1}	104, 90, 102	987	---
	10^{-2}	9, 16, 11	120	1.1×10^{4}
	10^{-3}	1, 1, 1	10	---
	10^{-4}	0, 0, 0	---	---
C-11	10^{0}	441, 456, 351	4160	---
	10^{-1}	56, 60, 48	547	---
	10^{-2}	3, 11, 7	70	4.2×10^{3}
	10^{-3}	0, 1, 0	3	---
	10^{-4}	0, 0, 0	---	---
D-10	10^{0}	134, 100, 104	1127	---
	10^{-1}	11, 4, 11	87	---
	10^{-2}	1, 1, 2	13	1.6×10^{3}
	10^{-3}	0, 1, 0	3	---
	10^{-4}	0, 0, 0	---	---

[a] Colonies per plate.

[b] Average number of colonies per milliter of sample.

[c] Colony forming units per milliter of Holston River Water.

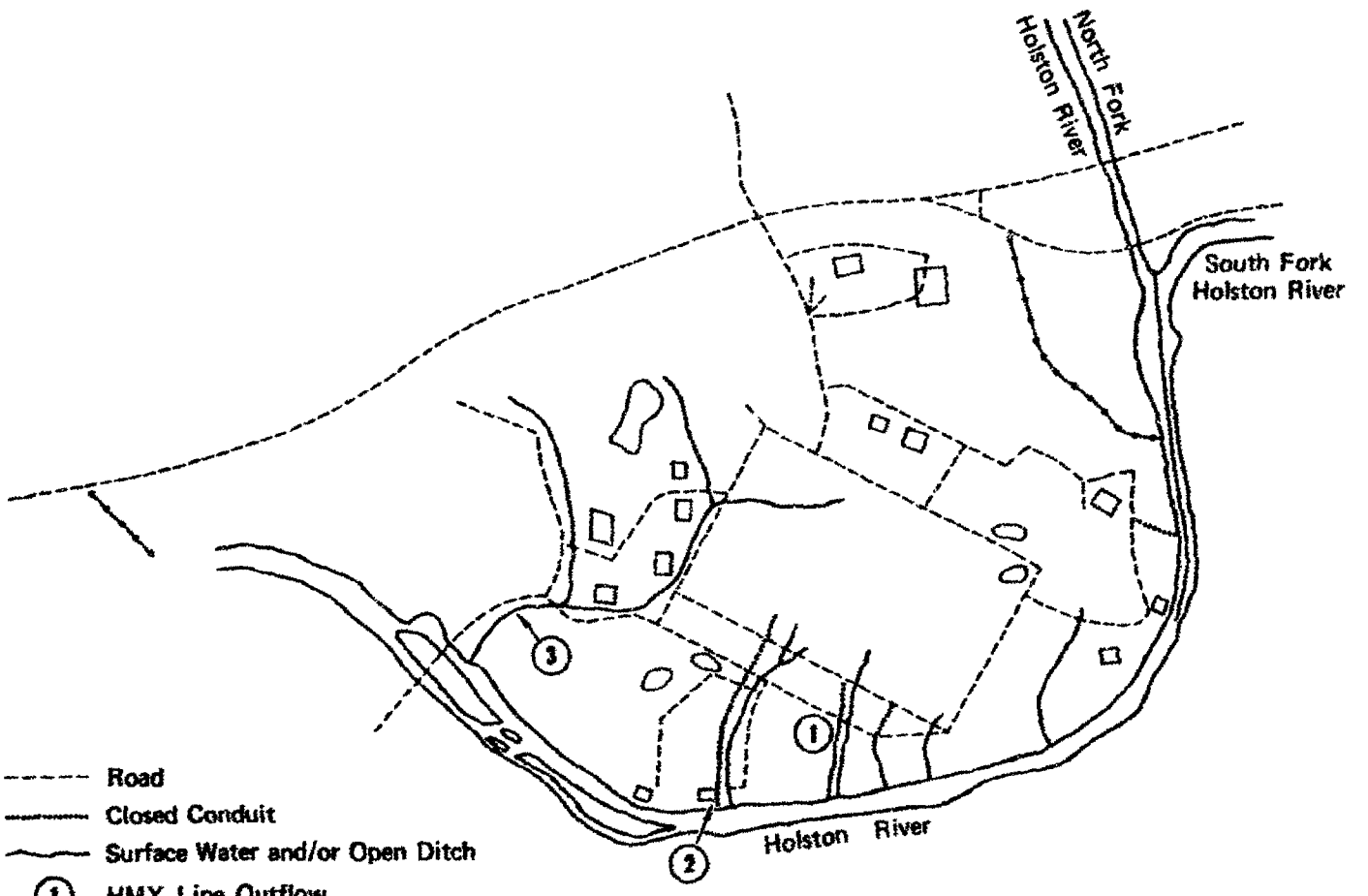

FIGURE 8 HOLSTON AAP – GENERAL LOCATION OF WASTE STREAMS

The HMX lines 1-7 are also underground until approximately 450 m from the Holston River, where the water surfaces, mixes with cooling water, and travels toward the river. The flow of the HMX lines 1-7 was not measured but estimated at 0.07 $m^3\ s^{-1}$. When mixed with cooling water, a stream approximately 1.5 m × 0.3 m is produced with an estimated velocity of 0.45 $m\ s^{-1}$.

Arnott Creek is approximately 7.6 m by 0.45 m and travels approximately 900 m to the Holston River. Wastes emptied into Arnott Creek are usually from building washout operations. The flow rate of the creek was estimated at 0.83 $m^3\ s^{-1}$.

The concentrations of TNT and RDX were determined for each wastestream by HPLC from samples taken midway between the plant and the Holston River in Arnott Creek and from the RDX and HMX lines prior to sunlight exposure. The input concentrations and mass calculations appear in Table 8.

Table 8

TNT AND RDX DISCHARGES INTO THE HOLSTON RIVER

Wastestream	Discharge Rate ($m^3\ s^{-1}$)	TNT		RDX	
		$mg\ l^{-1}$	$mg\ s^{-1}$	$mg\ l^{-1}$	$mg\ s^{-1}$
HMX lines 1-7	0.07	0.23	16.1	8.37	586
RDX lines 1-5	0.07	0.64	44.8	2.49	181
Arnott Creek	0.83	0.002	1.7	0.18	149

C. Rate and Equilibrium Constants

1. TNT Photolysis Rate Constant

To determine a photolysis rate constant for the TNT model simulation, we measured the sunlight photolysis rate constants of TNT in natural waters in several types of reaction cells and in the presence of suspended sediments to determine how these factors may affect photolysis rates.

To simulate an environmental situation in which sunlight irradiates a quiescent water body, we chose a flat-bottomed crystallizing dish 5 cm deep and 10 cm in diameter. Table 9 lists data on the photolysis of TNT in waters from the South Fork of the Holston River in open dishes and in a pyrex tube. The two dish experiments used filtered South Fork water in one dish and unfiltered water in the other dish, in which the sediment (collected with the sample) was kept in suspension by stirring. The photolyses were conducted on a clear sunny July day between 10:30 AM and 1:30 PM (high sun angle); therefore, the solutions in the dishes were irradiated through the surface of the water without any filtering of the light through glass.

Table 9

PHOTOLYSIS OF 0.61 ppm TNT IN NATURAL WATERS IN PRESENCE OF PARTICULATES AND IN SEVERAL TYPES OF REACTION CELLS[a]

Solutions and Conditions	Cell	Measured First-Order Rate Constants, k_p day^{-1}
Holston River water (South Fork), 0.2-) filtered	Tube	89
	Dish	26
Holston River water (South Fork), unfiltered and sediment suspended by stirring	Dish	18

[a]Photolyzed in July between 10:30 A.M.- 1:30 P.M.

The data show that photolysis of TNT in filtered natural waters occurs about 3.4 times faster in the tube than in the dish. The difference in these photolysis rate constants is mainly because of the greater light flux passing through the tube (360° exposure to light) than through the dish (light enters only from open top of dish).

The data in Table 9 for the Holston River water also indicate that in unfiltered waters containing sediment, the photolysis of TNT will be about 50% slower than that in filtered natural water. The slower photolysis rate is due both to light scattering and to light absorption by the particulates. Our understanding of the effects of particulates on photolysis rates in natural water is incomplete, but obviously such effects will be important in deep or turbid systems. Therefore, the maximum photolysis rate for TNT in the Holston River is expected to be 18 day^{-1} in July. Using the data of Zepp and Cline (1977) for light intensity in late spring (to correspond to field sampling dates), the photolysis rate constant reduces to 16 day^{-1}.

In our laboratory and sunlight photolysis studies of TNT, the experiments have been performed under conditions in which the solutions are optically "thin"; such solutions weakly absorb light with most incident light passing through. In deep aquatic system of some depth, however, light available for initiating reactions will decrease with increasing depth. Therefore, the photolysis rate of TNT will decrease with depth, and obviously no photolysis will occur below the level where all light is absorbed. Solutions in which most of the incident light is absorbed are referred to as optically "thick"; it should be noted that optically "thick" solutions may result from a long pathlength or a high absorption coefficient of the solution or both.

As an example of light penetration into a natural water, we have calculated the depth of Holston River water at which 99% of the incident light at the surface is absorbed. This situation occurs when the absorptivity of the water exceeds 2.0: that is when

$$\alpha_\lambda \times D > 2 \qquad (9)$$

where α_λ is the absorptivity at wavelength λ and D is the depth in centimeters. Table 10 lists the depths for several wavelengths in the solar spectrum.

Table 10

DEPTHS AT WHICH 99% OF LIGHT IS ABSORBED BY HOLSTON RIVER WATER[a]

Wavelength λ_1(nm)	Absorbance $\alpha_\lambda(cm^{-1})$	Depth (cm)
300	0.045	45
350	0.021	96
400	0.011	180
450	0.006	330
500	0.004	530

As these data show, the longer (and less energetic) wavelengths penetrate deeper into the Holston River water than do the shorter and more energetic wavelengths.

If sunlight were simply absorbed by the natural water without promoting the photolysis of TNT, the effect on the direct photolysis rate constant of TNT would be a straightforward light screening phenomenon that reduces the photolysis rate of TNT (Mill et al., 1981; Zepp and Cline, 1977). However, since light absorption by the natural water is responsible for the transformation of TNT, the estimation of the TNT loss rate due to photolytic processes is more complex.

As defined and developed in Part II-C of this report, Photochemical Studies of TNT in Natural Waters, the reaction quantum yield for indirect photolysis of TNT is given by Equation 10. Rearranging this equation gives the rate of loss of TNT:

[a]Sample taken in April, 1981.

$$\frac{-d(TNT)}{dt} = k_p[TNT] = \phi I\,[1-10^{-\alpha_\lambda \ell}]\,[TNT] \qquad (10)$$

As shown by the data in Table 11, the calculated ϕ values at 313 nm and 366 nm were roughly the same at the same initial TNT concentrations. Unfortunately, we could not perform enough experiments to determine at what longer wavelength the ϕ value would decrease such that photolysis rate of TNT would reach a limiting value (that is, at some less energetic wavelength, photolysis of TNT would be less efficient or not occur due to insufficient energy). More studies need to be performed before this approach to estimating TNT photolysis loss rates can be verified.

Table 11

QUANTUM YIELDS FOR TNT MEASURED IN SEARSVILLE POND WATER AT 313 NM AND 366 NM

$[TNT]_o$	λ(nm)	ϕ
2.79×10^{-6}	313[a]	8.8×10^{-4}
2.79×10^{-6}	366[b]	5.0×10^{-4}

An alternative procedure for calculating the photolysis rate constant of TNT in Holston River water (HRW; HRW* indicates an excited state) considers the following model scheme:

HRW → HRW*	k_a
HRW* + TNT → TNT products + HRW	k_r
HRW* → HRW	k_d

---

[a] $I_\lambda = 1.37 \times 10^6$ Einsteins ℓ^{-1} sec^{-1} at 313 nm
[b] $I_\lambda = 9.85 \times 10^6$ Einsteins ℓ^{-1} sec^{-1} at 366 nm

where k_a is the rate constant for light absorption by the natural water, k_r is the rate constant for production of products from reaction of TNT and HRW*, and k_d is the rate constant for decay of HRW*. The total rate of loss of TNT is defined by Equation 11,

$$\frac{-d(TNT)}{dt} = \frac{k_a k_r}{k_d} (TNT) = k_{pE}(TNT) \tag{11}$$

where k_{pE} is a first-order rate constant for loss of TNT.

Laboratory experiments that use 1-cm diameter tubes for photolysis give values of k_{pE} for optically thin natural water solutions (k_{pE}^{TN}) . The rate constant of interest for modeling the fate of TNT in deep aquatic systems is, however, that for the optically thick solution (k_{pE}^{TK}). The relationship between the two rate constants for midday sunlit conditions can be shown to be dependent only on the depth, D, and the α_λ values of the water body according to Equation 12,

$$\frac{k_{pE}^{TN}}{k_{pE}^{TK}} = 2.3\ D \frac{\Sigma \alpha_\lambda Z_\lambda}{\Sigma W_\lambda} \tag{12}$$

where α_λ is the midday sunlight intensity corrected for pathlength in a water body and W_λ is the midday sunlight intensity incident on the water-body. Values of Z_λ and W_λ, listed by Zepp and Cline (1977) for spring season dates at 40° latitude and 290 nm to 500 nm, were used at α_λ values measured for the Holston River water (South Fork), to calculate the value of Equation 13.

$$\frac{k_{pE}^{TN}}{k_{pE}^{TK}} = 0.022D \tag{13}$$

This equation indicates that for the spring season at midday and 40° latitude the two first-order rate constants are equal at a depth of 45 cm; in deeper waters k_{pE}^{TK} will be smaller than k_{pE}^{TN} .

To estimate a value of k_{pE}^{TK} for TNT for use in a fate model of the Holston River, we assumed an average river depth of 180 cm (6 ft), used a value of 16 day^{-1} for k_{pE}^{TN} as determined previously, and solved Equation 13 for k_{pE}^{TK} to yield an environmental photolysis rate constant of 4.0 day^{-1} at midday.

2. Other Rate and Equilibrium Constants

The remaining rate and equilibrium constants along with the TNT rate constant used in this study appear in Table 12. The sediment sorption partition coefficients were obtained from the Phase II study (Spanggord et al., 1980b). The biotransformation rate constant was also taken from the Phase II study; however, due to the observed low microbial counts, this constant was small compared to that for photolysis. The photolysis rate constant for RDX was also obtained from the Phase II study.

Table 12

RATE AND EQUILIBRIUM CONSTANTS FOR TNT AND RDX USED IN THE SRI MODEL

Chemical	Partition Coefficient	Photolysis (day^{-1})	Biotransformation (day^{-1})
RDX	5.0	0.1	—
TNT	50	16.4	0.03

D. Simulation of the One-Dimensional Compartmentalized River System

For the one-dimensional compartmentalized river system, the Holston River was divided into 67 compartments of equal length over the 33 km of the studied river reach. The reach was characterized as four different segments with each segment described by the geometric data surveyed at the sampling site. These characterizations are shown in Table 13.

Table 13

GEOMETRICAL INPUT DATA FOR THE ONE-DIMENSIONAL COMPARTMENTALIZED RIVER SYSTEM

Reach	Compartments	Volume (ℓ)	Settling Rate (% day^{-1})	Scouring Rate (% day^{-1})
1	1 to 9	1.0×10^8	0.82	2.0×10^{-4}
2	10 to 18	1.3×10^8	0.64	2.0×10^{-4}
3	19 to 40	0.8×10^8	0.64	2.0×10^{-4}
4	41 to 67	1.4×10^8	0.80	1.4×10^{-4}

The settling rate in each segment was estimated from the suspended sediment measurements made at each site. We assumed that the sediments were in equilibrium during the simulation period. The scouring rate was estimated by assuming that 1% of the suspended solids were returned to the aqueous phase from the bottom sediment.

RDX was selected for the initial investigation of the one-dimensional system because RDX is a relatively conservative chemical, and therefore, the mixing and dilution properties of the Holston River could be evaluated. The RDX loadings from the HMX lines, RDX lines, and Arnott Creek were entered into compartments 1, 2, and 7, respectively. The concentration-time (distance) dependent profile of RDX predicted by the one-dimensional system appears in Figure 9.

At Site A, the predicted RDX concentration is 8.0 ppb. The actual values found ranged from 212 ppb (North Bank) to less than 1.0 ppb on the South Bank (see Section IV-G). The actual values found across the width of the river indicate that the Holston River is not well mixed. Since the one-dimensional system assumes a well-mixed reaction vessel, the application of the model before the river becomes homogeneous will lead to erroneous predictions. The predicted and observed values of RDX at each sampling site appear in Table 14.

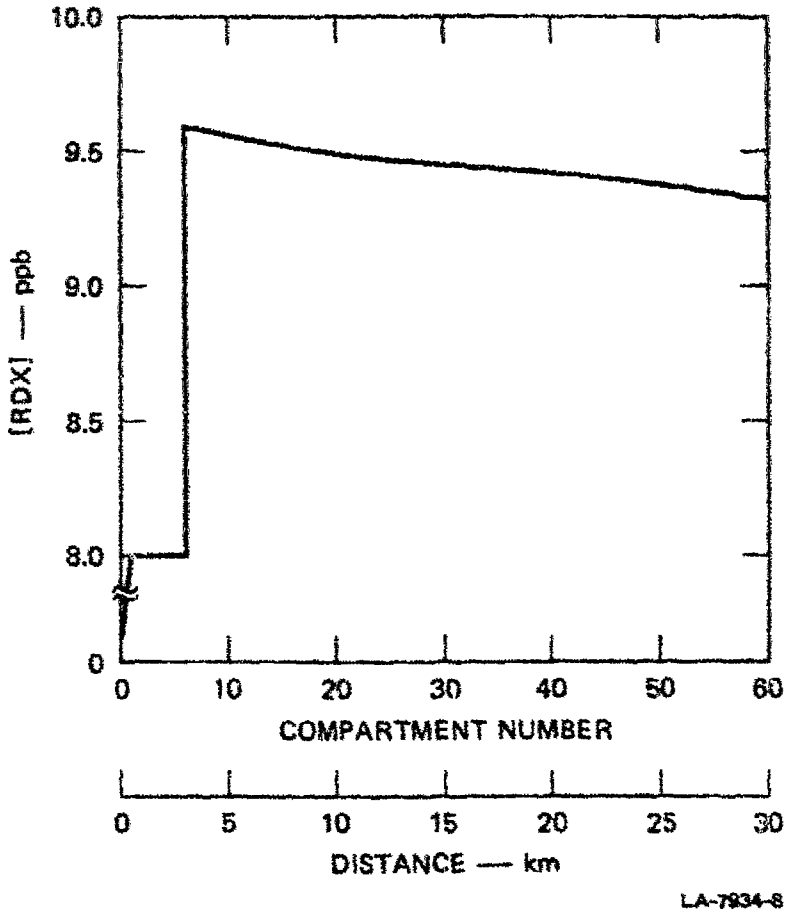

FIGURE 9 RDX CONCENTRATION PROFILE IN THE HOLSTON RIVER PREDICTED BY ONE-DIMENSIONAL MODEL

Table 14

ONE-DIMENSIONAL COMPARTMENTALIZED RIVER SYSTEM
PREDICTIONS AND FOUND CONCENTRATIONS OF
RDX IN THE HOLSTON RIVER

Site	Predicted Concentration(ppb)	Found Concentration(ppb)		
		North Bank	Middle	South Bank
A	8.0	212.	1.27	0.5
B	9.6	7.3	12.3	4.1
C	9.5	12.5	10.3	4.6
D	9.3	9.7	7.1	7.6

From the observed concentrations of RDX, it is clear that homogeneity in the Holston River is eventually achieved somewhere between Sites C and D. At Site D, where homogeneity is achieved, the predicted value is in good agreement with the observed value.

E. Simulation of the Two-Dimensional Compartmentalized River System

Since the one-dimensional compartmentalized river system could not adequately describe the concentration profile of RDX near the discharge sites, we employed a two-dimensional compartmentalized river system that considers both lateral and directional flows to describe the loss and movement of TNT and RDX in the Holston River.

1. Compartmentalization and Lateral Flow

The Holston River was compartmentalized as shown in Figure 10, where the left-hand compartments represent the North Bank and the right-hand compartments represent the South Bank. In the two dimensional compartmentalized river system, the chemicals introduced into compartment 1 are allowed to move laterally into compartment 2 as well as in the direction of the river flow (compartment 4). The HAAP discharge lines enter the two-dimensional compartmentalized river system at compartments 1 (HMX lines 1-7), 4 (RDX lines 1-5), and 16 (Arnott Creek). The lateral flow was estimated from the dye studies of Sullivan et al. (1977) who

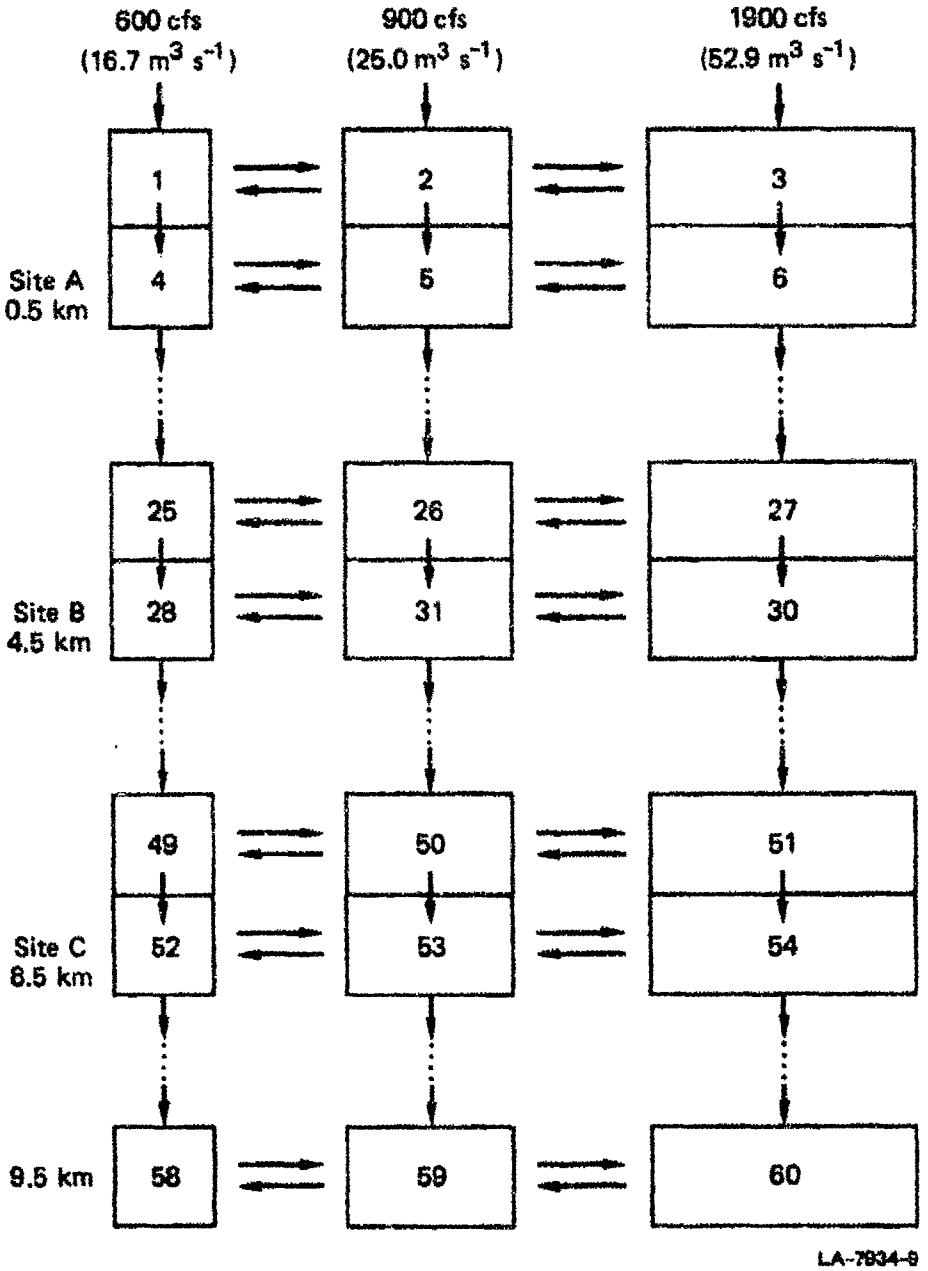

FIGURE 10 MODEL SIMULATION OF COMPARTMENTS REPRESENTING HETEROGENEOUS MIXING

determined that discharges from the RDX lines 1-5 would not become homogeneous until 10 km from the discharge point (with an instream flow of 223 m^3 s^{-1}). Assuming an average flow velocity of 0.43 m s^{-1}, we calculated it would take 6 hours for water to traverse 10 km and therefore 6 hours to traverse the width of the river. Therefore, for Sullivan's study, we can estimate the lateral flows at Sites A, B, and C to be 4.5×10^{-3} m^3 s^{-1}. During the field study, the instream flow was only 95 m^3 s^{-1}, or approximately half of that observed by Sullivan. We therefore assumed that our lateral flow velocities would be half of those observed by Sullivan and that homogeneity of the Holston River would not be achieved until 20 km downstream from the discharge point. After 20 km, the one-dimensional compartmentalized river system was employed for the remainder of the river reach.

2. Cross-Sectional Area of Each Compartment

To determine the cross-sectional area of each compartment, we plotted the cumulative flow against the cumulative cross-sectional area from the data collected by the USGS at each site (Table 1). This plot appears in Figure 11. We arbitrarily divided the river into three lateral compartments with flows of 16.7, 25.0, and 53 m^3 s^{-1} in the transect direction. We then computed the cross-sectional area and flow velocity for each compartment; these data are listed in Table 15. These data show a greater flow in the center of the river, which is consistent with the observed results.

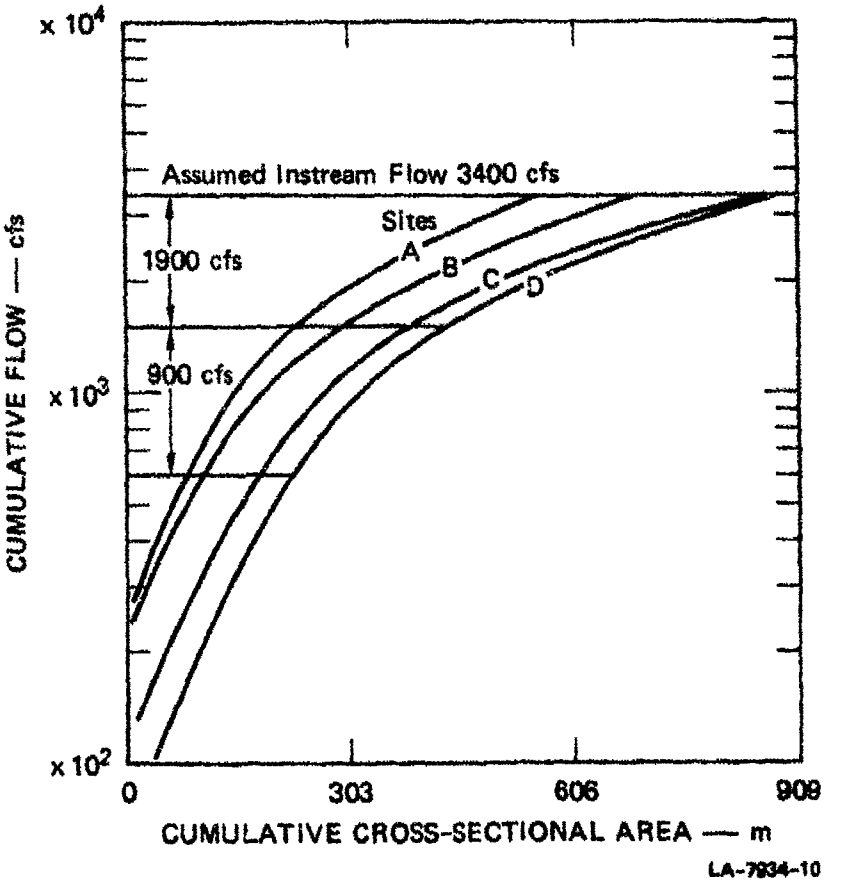

FIGURE 11 RELATIONSHIP OF CUMULATIVE FLOW TO CUMULATIVE CROSS-SECTIONAL AREA

Table 15

CROSS-SECTIONAL AREAS AND FLOW VELOCITIES OF LATERAL COMPARTMENTS AT SITES A, B, AND C

Site Flow ($m^3\ s^{-1}$)	A X-Area (m^2)	A Velocity ($m\ s^{-1}$)	B X-Area (m^2)	B Velocity ($m\ s^{-1}$)	C X-Area (m^2)	C Velocity ($m\ s^{-1}$)
16.7	36.7	0.46	55	0.30	27.5	0.61
25.0	50.5	0.50	60	0.42	41.3	0.61
53.0	119.4	0.44	147	0.36	99.2	0.53

3. RDX Simulation

The results for the simulation of RDX concentrations are shown graphically for the North Bank, Center, and South Bank of the Holston River in Figure 12. The profiles indicate that the North Bank undergoes continuous dilution until homogeneity in the river is achieved at 20 km. The concentration of RDX in the center of the river increases, exceeds a downstream homogeneous concentration, then tapers off to a constant value (homogeneity). The South Bank RDX concentration increases continually until homogeneity is achieved. The transport (sorption) and transformation (photolysis) processes have little effect on reducing the RDX concentration over the studied river reach. For example, the RDX concentration at 20-km, 9.2 ppb, will decrease to 9.0 ppb at Site D. We expect only 5% of the RDX to be transformed over 33 km. Therefore, in the case of RDX, the two-dimensional compartmentalized river system describes the dilution and mixing properties of the Holston River.

F. TNT Simulation Employing a Two-Dimensional Compartmentalized River System

Using the input concentration of TNT found at Site A-1, we ran the TNT simulation two-dimensional compartmentalized river system using photochemical rate constants of 4 and 16 day^{-1}. The concentration-time-of-day-dependent curves for each rate constant appear in Figure 13 and 14

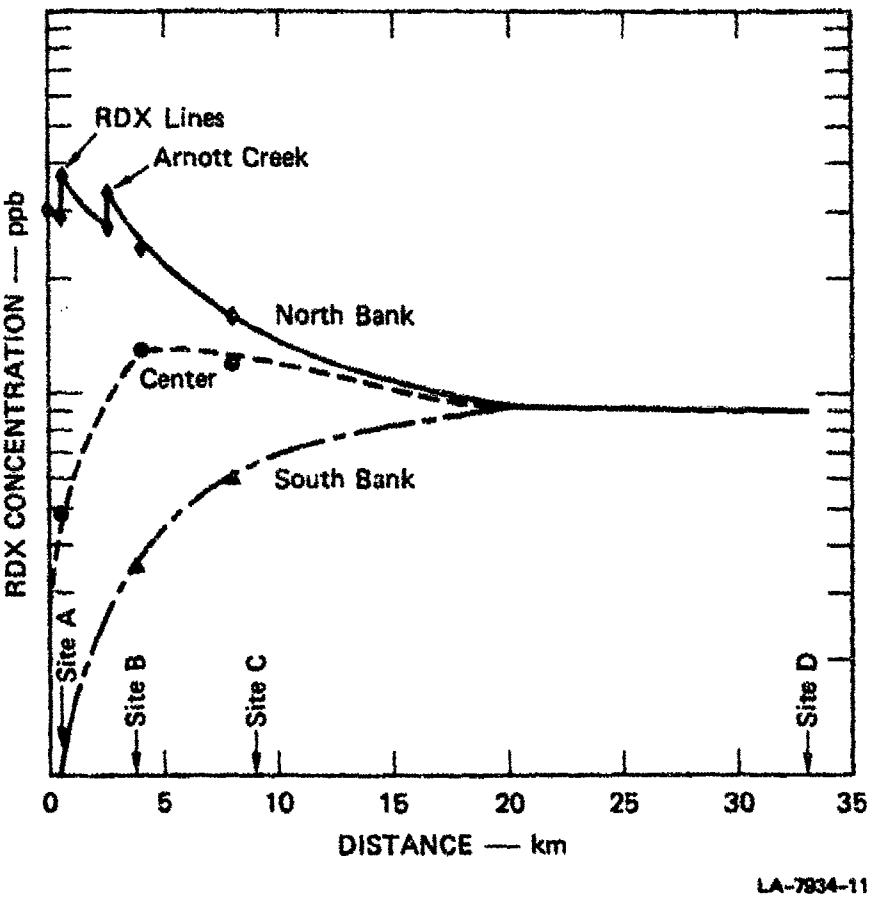

FIGURE 12 PREDICTED RDX CONCENTRATION PROFILE IN THE HOLSTON RIVER COMPUTED FROM THE TWO-DIMENSIONAL MODEL

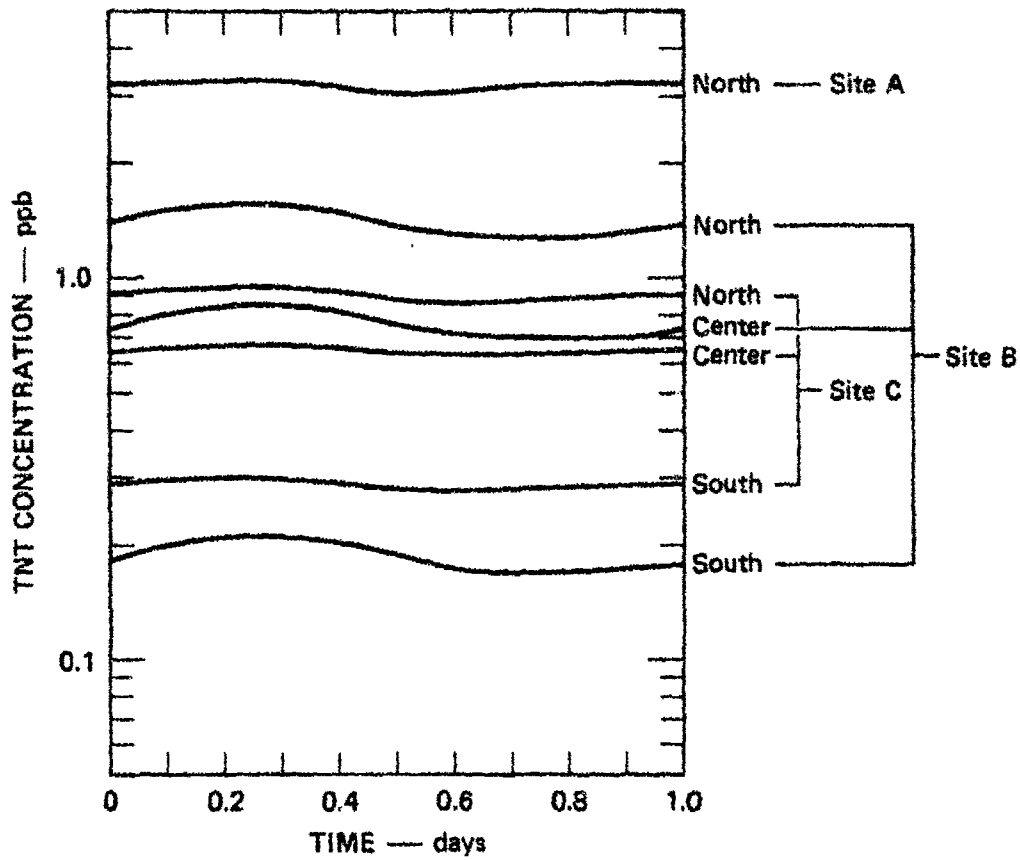

FIGURE 13 TNT CONCENTRATION AS A FUNCTION OF TIME OF DAY USING A PHOTOLYSIS RATE CONSTANT OF 4 DAY^{-1}

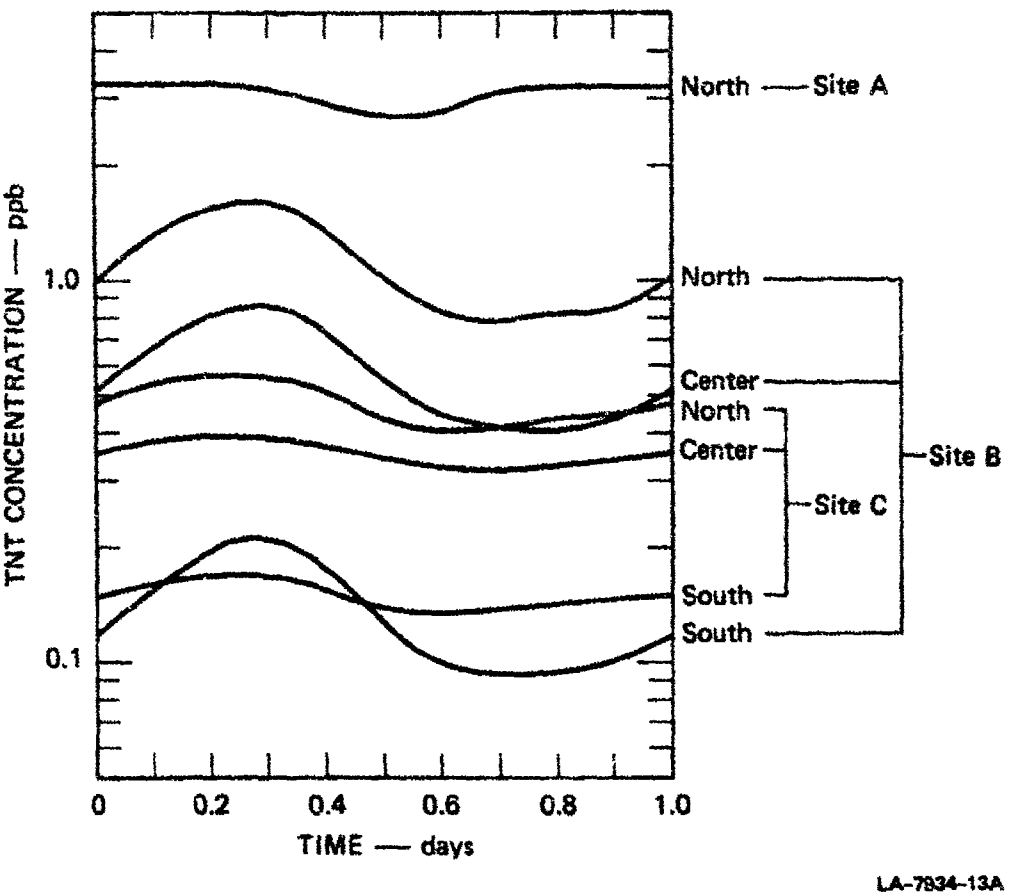

FIGURE 14 TNT CONCENTRATION AS A FUNCTION OF TIME OF DAY USING A PHOTOLYSIS RATE CONSTANT OF 16 DAY^{-1}

for the North Bank of Site A and the North, Center, and South Banks of Sites B and C. These curves readily show the TNT concentration dependence on the photochemical rate constant. Although the value of 4 day^{-1} was used in this study (as determined from the laboratory studies), this value was generated from highly turbid waters due to rains and runoff in the area. We expect, therefore, that under less turbid conditions, the photochemical rate constant may rise to 16 day^{-1} or above in the Holston River.

Using the photochemical rate constant of 4 day^{-1}, the predicted profile of TNT concentration as a function of distance from the discharge point is shown in Figure 15 for the North, Center, and South portions of the Holston River at noontime. The curves are highly divergent at Site A due to poor mixing, and follow a similar pattern to that of RDX (Figure 12). The curves converge at 20 km (homogeneity), then decrease as a function of the photochemical rate constant. We expect that TNT concentrations near the plant boundary (8 km) are primarily controlled by dilution under the conditions of this study.

G. Monitoring Data From The Holston River

The concentrations of munitions-related pollutants being discharged into the Holston River were determined by HPLC as described in Section III. The components were identified by their capacity factors as compared to authentic standards. The chromatographic profiles for all the analyzed samples appear in Appendix 1. We observed that the chromatographic profiles became complex close to the South Bank. This probably results from wastes discharged from upstream industries located on the South Fork of the Holston River. In some chromatograms the waste products coeluted with our internal standard. We therefore calculated the concentration of the munitions-related pollutants by both internal and external standard methods. The observed concentrations of SEX, TAX, HMX, RDX, and TNT at each site and section appear in Table 16.

The data indicate that at Site A, most of the discharge is hugging the North Bank with little dispersion into the river. At Sites B and C, the lateral transport of chemical becomes evident, and at Site D, complete mixing of the river has been achieved. The dispersion phenomenon is depicted in Figure 16 for RDX.

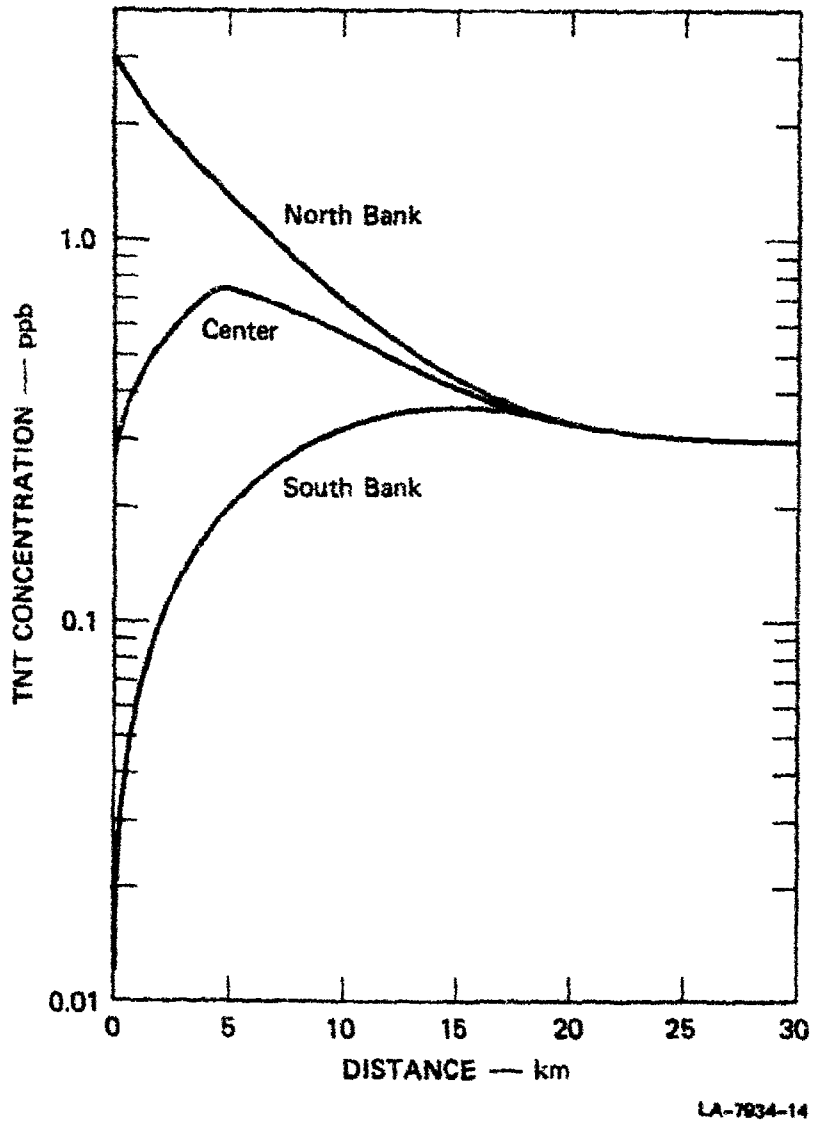

FIGURE 15 TNT CONCENTRATION AT NOON AS A FUNCTION OF DISTANCE FROM THE DISCHARGE POINT FOR THE NORTH, CENTRAL, AND SOUTH PORTIONS OF THE HOLSTON RIVER

Table 16

CONCENTRATIONS OF (µg/ℓ) OF SEX, TAX, HMX, RDX, AND TNT FOUND IN THE HAAP DISCHARGE LINES AND AT VARIOUS SITES IN THE HOLSTON RIVER

Site	SEX		TAX		HMX		RDX		TNT	
	I.S.	Ex. S.	I.S.	Ex. S.	I.S.	Ex. S.	I.S.	Ex. S.	I.S.	Ex. S.
RDX 1-5	774	764	505	498	59.4	58.4	2596	2565	645	637
HMX 1-7	1687	1696	3164	3180	10.6	11.3	8321	8370	234	235
Arnot Creek[a]	1.6	1.8	74.3	82.5	4.24	4.67	177	196		
RDX 1-5 w/H_2O	198	216	449	211	14.9	16.2	709	773	111	121
					7.43	7.53	234	213	333	3.45
A1 (Site A,							2.61	2.50	0.22	0.21
A2 0.1 km)	9.13	8.93	4.46	4.31			2.50	3.75	0.44	0.67
A3	2.18	3.18	1.93	2.82			0.44	0.49		0.02
A4			1.05	1.14			2.40	2.41		
A5			1.93	2.80	0.11	0.11	1.93	1.93		
A6			1.05	1.05			0.67	0.68	0.01	0.01
A7			0.91	0.92			0.21	0.23		
A8[a]			0.31	0.34			1.27	1.27		
A9			1.01	1.01			0.29	0.27		
A10			0.68	0.64			1.07	1.53		0.02
A11			1.05	0.95			0.41	0.38		
A12			0.62	0.58			0.81	0.87		0.02
A13			0.49	0.52			1.47	1.49		
A14			0.33	0.33			3.04	3.62		
A15[a]			2.14	2.56			0.46	0.50		
A16			2.27	2.46			2.23	2.90		
A17	0.57	0.75	1.22	1.59						
A18[a]										
A19[a]	0.48	0.93	0.74	1.47						
A20[a]										
A21[a]	0.52	1.01	0.92	1.74						
B1 (Site B,	3.76	3.61	7.28	7.01	0.24	0.23	17.3	16.7	0.05	(0.05)
B2 4 km)	4.98	4.96	5.56	5.53	0.22	0.22	17.9	17.8		(0.04)
B3	5.87	5.60	6.19	5.90			23.8	22.7		(0.05)
B4	6.54	6.80	6.92	7.19			21.6	22.4		(0.05)
B5	6.26	5.77	7.74	7.13			22.6	20.9		(0.05)
B6	7.28	7.36	5.45	5.51			20.4	20.8		(0.04)
B7	6.41	7.06	5.87	5.30			18.9	20.5		0.09
B8	5.67	5.41	5.61	3.45			15.0	14.4		0.17
B9[a]	5.67	6.28	4.19	4.65			14.5	16.1		0.09
B10	5.87	6.32	3.78	3.53			12.3	13.1		0.17
B11	4.01	4.12	3.61	3.71			11.1	11.4		(0.02)
B12[a]	2.87	3.33	3.05	3.54			8.79	10.2		
B13	3.41	3.43	2.91	2.92			9.34	9.41		(0.01)
B14[a]	2.67	3.23	1.83	2.20			6.97	8.35		
B15[a]	2.08	2.34	2.59	2.87			8.15	9.05		
B16	1.58	1.72	3.05	3.31			5.03	5.48		
B17	1.72	1.69	2.73	2.67			6.90	6.74		
B18	1.19	1.21	1.89	1.92			5.22	5.31		
B19[a]	0.93	1.37	1.28	1.83			3.08	4.52		
B20[a]	0.71	0.97	1.10	1.49			2.96	4.09		

Table 16 Concluded)

Site	SEX		TAT		MUX		RDX		TNT	
	I.S.	Ex. S.	I.S.	Ex. S.	I.S.	Ex. S.	I.S.	Ex. S.	I.S.	Ex. S.
B21[a]	1.03	1.40	1.50	2.14			4.28	5.82		
B22	0.81	1.21	0.92	1.37			2.53	3.73		
B23[a]	0.75	1.05	1.14	1.58			3.24	4.48		
B24[a]	12.5	19.6	11.0	17.4			6.49	10.3		
C1 (Site C, 8 km)	3.41	3.59	4.29	4.52	0.29	0.30	12.5	13.1	.008	(0.04)
C2	3.31	3.59	4.77	5.16			14.7	15.8		
C3	3.13	3.41	5.36	5.83			13.8	15.0		(0.05)
C4	3.49	3.79	5.90	6.40			15.2	16.6		
C5[a]	2.60	3.49	5.22	7.00			13.0	17.4		(0.06)
C6	3.37	3.49	7.57	7.80			14.6	15.0		
C7[a]	2.62	3.06	5.45	6.37			10.6	12.4		
C8	2.98	3.23	6.43	7.00			11.6	12.6		(0.01)
C9	2.44	2.56	5.92	6.23			10.6	11.1		(0.01)
C10	2.00	2.08	5.50	5.77			10.3	10.6		
C11[a]	1.51	2.06	3.40	4.64			5.89	8.02		(0.07)
C12[a]	1.57	1.39	4.73	4.20			9.65	8.59		(0.06)
C13	1.07	1.15	3.36	3.62			6.85	7.40		(0.03)
C14[a]	0.91	1.11	2.74	3.36			4.54	5.55		(0.05)
C15[a]	0.69	0.89	1.88	2.41			4.01	5.10		(0.01)
C16[a]	0.71	0.81	2.18	2.50			4.00	4.56		(0.07)
C17[a]	0.65	0.95	1.49	2.11			3.26	4.62		(0.03)
C18	0.91	0.83	2.10	1.92			4.44	4.08		(0.04)
D1 (Site D, 33 km)	2.34	2.48	5.35	5.66			7.47	7.91		(0.07)
D2										
D3[a]	1.13	1.34	4.03	4.80			5.83	6.83		(0.03)
D4	1.37	1.49	3.92	3.71			6.91	6.53		(0.03)
D5[a]	1.17	1.47	3.13	3.95			5.87	7.39		(0.02)
D6[a]	2.03	1.98	4.63	4.01			7.43	6.42		(0.02)
D7[a]	1.45	1.82	3.31	4.18			4.99	6.30		(0.04)
D8	1.49	1.49	3.91	3.91			5.49	5.51		
D9[a]	0.99	1.53	2.96	4.59			4.59	7.11		(0.02)
D10	1.92	1.96	4.86	4.95			5.84	5.94		(0.04)
D11[a]	1.34	2.02	3.41	5.10			5.18	7.73		(0.02)
D12	1.55	1.61	4.29	4.59			6.20	6.47		
D13[a]	1.81	2.00	6.06	6.72			5.76	6.38		(0.04)
D14	2.18	2.32	4.42	4.70			6.42	6.81		
D15	1.33	1.41	2.70	2.87			3.67	3.89		
D16	2.20	2.28	4.62	4.80			6.92	7.19		
D17	2.24	2.32	5.26	5.43			7.74	8.01		(0.01)
D18	2.28	2.48	4.22	4.63			7.99	8.76		
D19[a]	1.71	1.92	4.96	5.60			6.62	7.42		(0.01)
D20[a]	2.08	2.34	4.73	5.30			6.80	7.63		

[a]Extracts in which interferences caused integration of the internal standard to deviate > 10% of expected value.

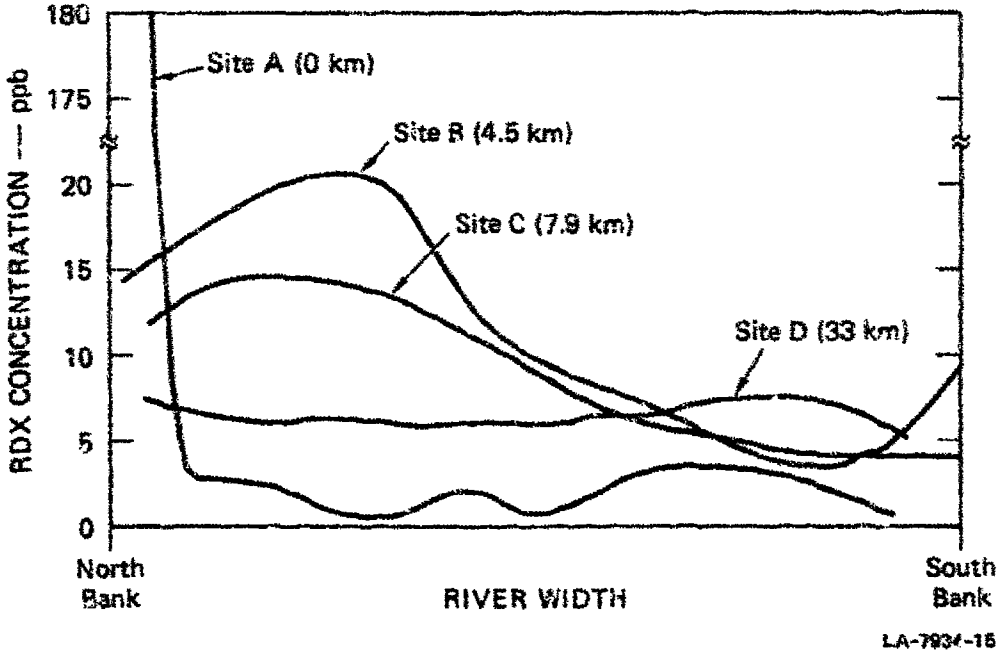

FIGURE 16 PROFILE OF RDX CONCENTRATIONS AT SAMPLING SITES A, B, C, AND D

The data also show that little TNT and HMX were being discharged during the day of sample collection (April 22). At all four sites, many of the TNT analysis values were at background levels. This background concentration averaged to 0.03 ppb. Random GC-ECD analyses of sample extracts confirmed the presence of TNT, but these results could not be confirmed by mass spectrometry.

Due to the rapid transformation of TNT in the environment and the large dilution factors caused by heavy flow, TNT could be detected only at a few locations. The paucity of analytical data was sufficient to hinder rigorous validation of the SRI Model using TNT.

H. Sediment Analyses

The sediment extracts were analyzed by HPLC as previously described. Very large peaks eluted with retention volumes similiar to those of SEX, TAX, and HMX, and the presence or absence of these compounds was not confirmed. RDX was identified in the sediments along with 4-amino-2,4-dinitrotoluene and 2-amino-4,6-dinitrotoluene. The identification of the latter two compounds was confirmed by probe mass spectrometry of samples collected from the HPLC. A chromatographic profile of Site A sediment appears in Figure 17 and the amounts of RDX, 4-A-2,6-DNT, and 2-A-4,6-DNT appear in Table 17. The amounts of amino-dinitrotoluenes in the sediment extracts were confirmed by GC-ECD and GC-MS.

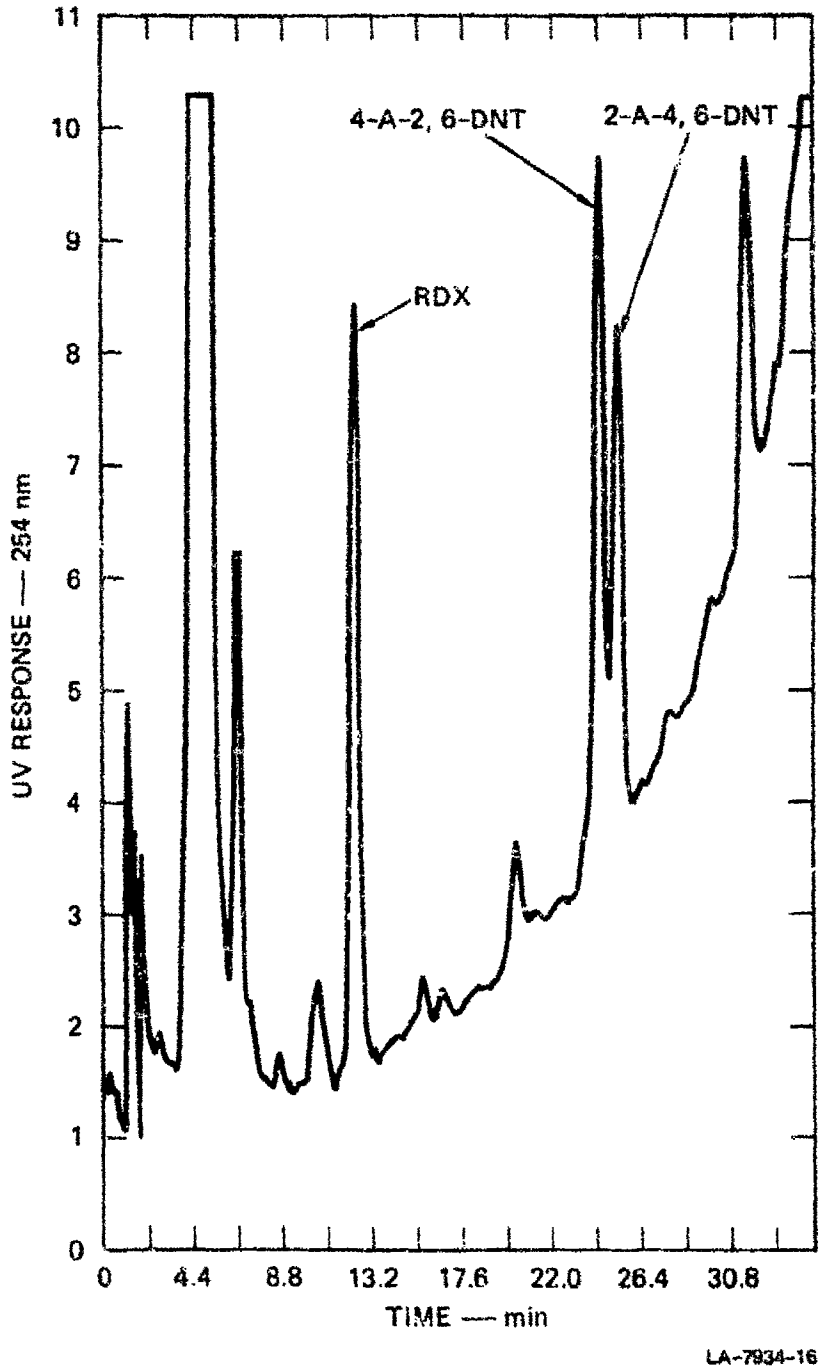

FIGURE 17 HPLC PROFILE OF SITE A SEDIMENT EXTRACT

Table 17

CONCENTRATIONS OF RDX, 4-A-2,6-DNT,
2-A-4,6-DNT FOUND IN HOLSTON RIVER SEDIMENT

Site	RDX (ng g^{-1})	4-A-2,6-DNT(ng g^{-1})	2-A-4,6-DNT(ng g^{-1})
A	358	97.3	67.5
B	--	18.0	3.1
C	--	0.8	0.4
D	--	<0.3	--

RDX was found only in Site A sediment near the RDX lines 1-5 outflow. No partitioning of RDX to the sediment was observed further downstream. No TNT was observed at any site in the sediment, but the major biological transformation products, the aminodinitrotoluenes, were observed. The amounts found indicate that at least 189 ng g^{-1} of TNT were sorbed at Site A, 24.2 ng g^{-1} at Site B, 1.4 ng g^{-1} at Site C, and less than 0.3 ng g^{-1} at Site D. Our Phase II studies indicated that TNT would transform rapidly in the presence of high microbial populations and added organic nutrient. Therefore, it is not surprising to observe this transformation. In the aqueous phase, however, we believe biologic transformation is nil because of the low microbial population.

I. Comparison Of Actual RDX Concentrations To Those From The Simulation of the Two-Dimensional Compartmentalized River System

The predicted and actual concentrations of RDX found along the North Bank, Center, and South Bank of the Holston River appear in Table 18.

Table 18

PREDICTED AND ACTUAL CONCENTRATIONS (ppb) OF RDX DETERMINED IN THE HOLSTON RIVER

	North Bank		Center		South Bank	
Site	Predicted	Avg. Found	Predicted	Avg. Found	Predicted	Avg. Found
A (0.1 km)	37.0	55.0	4.8	1.0	0.028	0.090
B (4.5 km)	24.0	20.1	13.0	16.0	3.5	7.2
C (7.9 km)	16.0	14.1	12.0	12.0	6.0	6.0
D (33.0 km)	9.0	6.5	9.0	6.5	9.0	6.5

At Site A, the found RDX concentration on the North Bank is higher than the predicted value because a very high RDX concentration hugs the North Bank. The higher predicted RDX concentration in the center of the river and the predicted lower concentration at the South Bank indicate that the predicted lateral dispersion is faster than the actual rate at Site A.

At Site B, the higher predicted North Bank RDX concentration and the lower predicted Center and South Bank RDX concentrations indicate that the predicted lateral dispersion is beginning to approximate the actual value.

However, at Site C, the predicted and actual values agree quite closely, indicating that the lateral flow rate has increased between Sites B and C. This is expected, since Site C is much shallower than Site B (1.4 m versus 2.5 m).

At Site D, the one-dimensional compartmentalized river system has been employed for 13 km, and complete mixing of the river is predicted. The actual values confirm the river's homogeneity; however, they are slightly lower than the predicted values. Part of the difference is attributable to further dilution from small input streams, surface runoff (rain occurred the night before the sampling at Site D), and rain.

The actual values demonstrate that lateral dilution is the controlling factor in predicting the RDX concentration at locations near the HAAP. Once the river reaches a steady state, we expect that the RDX concentration will remain constant at any time of the day as long as environmental conditions are constant. Dilution, therefore, is the primary factor in controlling the RDX concentration in the Holston River, and this phenomenon can adequately be described by the two-dimensional compartmentalized river system.

J. Comparison Of Actual TNT Concentrations To Those From The Two Dimensional Compartmentalized River System

As stated previously, the low discharge level of TNT and the dilution of wastestreams by the Holston River prevented the collection of reliable analytical data for model validation. However, since the two-dimensional compartmentalized river system could adequately describe the dilution processes in the Holston River, we can compare a few of the data points found at Site B with those predicted by the model simulation.

The Table 15 data indicate low (0.05 ppb) TNT concentrations along the North Bank (Sites B-1 to B-4) increasing to 0.17 ppb near the center of the river. The simulation results indicate concentrations of 1.4 ppb on the North Bank and 0.75 ppb in the center of the river during the time of sampling (12:00 P.M.). The much lower found values compared to the predicted values on the North Bank could arise from several factors. One is that the velocity of the water on the North Bank is much slower than the velocity in the center of the river. On a comparative basis for waters traveling between points A and B, water near the banks travels much slower than water in the middle of the river. The longer residence time between the two points allows more transformation to occur, thus producing TNT concentrations lower than those observed in the center of the river. In the model simulation, average river flow velocity is used. Thus, for accurate modeling of the North and South Banks, actual flow velocities along these banks should be used.

A second factor contributing to higher model-predicted values on the North Bank is the use of an average river depth value in the calculations of the photochemical rate constant. Since the North Bank waters begin at "zero" depth and increase to an "average" depth, within this zero-to-average depth range, the photochemical rate constant is higher than the value used in the model simulation. Therefore, the simulation model will again predict higher values than those observed. This can be corrected in the model by using photochemical rate constants determined from shallower depths.

In the center of the river, the predicted value (0.75 ppb) and the actual value (0.17 ppb) differ by approximately a factor of four. This may indicate that the model simulation is beginning to approximate the transformation processes in the Holston River; more data points are necessary to confirm this expectation. In any case, a factor of four may be a reasonable value when modeling real world environments.

K. Persistence of SEX, TAX, and HMX in the Holston River

During the field study, SEX, TAX, and HMX were being discharged simultaneously with TNT and RDX. The HMX concentrations in the discharge lines were low (4 to 60 ppb) and dilution from the Holston River reduced the concentration of this component to below detection limits.

SEX and TAX, however, were observed at all sampling sites. Their concentration profile paralleled that of RDX (Figure 12) and indicated river homogeneity at Site D. From the available data, it appears that SEX and TAX will be persistent chemicals in the aquatic environment.

V DISCUSSION

The results of this study indicate that the SRI model can be used as a predictive tool to estimate the concentrations of TNT and RDX in the Holston River. The SRI computer model proved to be reliable (factor of 1.5) for estimating RDX concentrations in the one-dimensional compartmentalized river system at distances beyond 20 km from the discharge point or at locations where river homogeneity has been achieved. However, due to the incomplete mixing of the Holston River at locations near the discharge points, the one-dimensional compartmentalized river system could not be used because a basic assumption within the model considers the river compartment a well-mixed reaction vessel. Since the transformation processes that affect the persistence of TNT had lowered the TNT concentration below detection limits before river homogeneity could be achieved, the one-dimensional model was not applied to TNT.

Because of the incomplete mixing of the Holston River near HAAP, a two-dimensional compartmentalized river system was developed that took into account the lateral dispersion of water across the Holston River. When this model was applied to RDX, the predicted RDX concentrations in the North, South, and Center portions of the Holston River were in good agreement with the actual values. Since RDX is a conservative chemical, the two-dimensional compartmentalized river system adequately describes the dilution of RDX in the nondispersed reach of the Holston River. The nondispersion effect is dependent on the total river flow velocity and the SRI model can be adjusted easily to account for this effect.

Validation of the SRI model using TNT was prevented by the low input concentrations of TNT during the field study and the poor dispersion of the effluent stream from RDX lines 1-5 into the Holston River. The data from the analysis of water samples showed little penetration of TNT into the middle of the river and indicated that a rapid transformation of TNT was occurring along the North Bank. The transformation rate appeared to be more rapid than that which could be estimated by the model simulation.

This discrepancy could be accounted for by the North Bank waters moving at a much slower rate than the rate that was measured at station A-1, 25 feet from the shore (1.78 $m^3\ s^{-1}$). Since the two-dimensional system predicted an RDX concentration of 37 ppb at station A-1 and 212 ppb was found, we know that the lateral dispersion at station A-1 was greatly overestimated. This indicates that the RDX lines 1-5 wastewaters are close to the North Bank at station A-1 and are moving at a flow between 0 (shoreline) and 1.78 $m^3\ s^{-1}$. Thus, the residence time of TNT (and RDX) in the North Bank compartments may actually be longer than estimated with the available data. Model validation could be achieved with TNT by allowing a 24-hour continuous discharge through RDX lines 1-5 and by beginning to collect samples at 6:00 AM at Site C followed by successive sampling at locations downstream. In this way we would obtain better analytical data at higher concentrations of TNT with which to compare with the predicted values.

We did, however, obtain sufficient data to estimate a transformation rate constant for TNT between Sites A and B. RDX was used as a marker compound to estimate the lateral dilution factor between Sites A and B. This factor was calculated to be 10.4. The initial TNT concentration at Site A (3.3 ppb) is expected to decrease to 0.31 ppb in the absence of transformation. Since a TNT concentration of 0.17 ppb was found at Site B (4.5 km), we estimated that 0.14 ppb of TNT underwent transformation. The observed transformation rate constant was estimated as follows:

$$\ln\frac{C_o}{C} = k_p t$$

$$\ln\frac{0.31}{0.17} = k_p(0.115\ \text{days}) \qquad (14)$$

$$5.2\ \text{day}^{-1} = k_p$$

If we assume an average depth of 1.8 m between sites A and B and use the thin film-thick film theory to correct for depth, the expected photoysis rate constant should be

$$k_p^{TK} = \frac{16\ day^{-1}}{(0.022)\ (180cm)} = 4.0\ day^{-1} \quad (15)$$

which is in good agreement with the measured value.

These results suggest that the laboratory measurement of k_p can be used reliably to estimate a value in the river. The good agreement between values of k_p also indicate that other processes such as biotransformation are not occuring to any extent. Biotransformation did occur in the sediment; however, due to the low microbial population in the river, this process is not believed to be occurring to any extent in the major portion of the river. Biotransformation may occur in isolated pools, but the overall loss would not be observed in the river.

That no TNT is found in the sediments suggests that biotransformation is rapid in this compartment. How this affects the sorption partition coefficient for TNT is not known at this time. The sediment loading of TNT transformation products does decrease between Sites A and D, which reflects the lower aqueous-phase concentration of TNT reaching the downstream site.

A number of assumptions used in this study deserve further comment. First, we have assumed that homogeneity of the Holston River will be achieved at 20 km for the given flow rate. The predicted and observed values for RDX at Site C are in reasonable agreement, which indicates that this was a good assumption. However, the observed and predicted value at Sites A and B may have been in better agreement if lateral transport was reduced. Thus, for predicting pollutant concentration, the dependence of complete mixing (homogeneity) on flow rate should be better understood for modeling purposes.

Second, we have assumed pseudo-first-order kinetic behavior for the photolysis of TNT. Our studies have shown that the photolysis depends on other species in natural waters (such as humic acids), and the exact

kinetic dependence is unknown. This added complexity may cause some variation in the pseudo-first-order rate constant at different sampling locations. The magnitude of error resulting from this assumption is unknown.

The environmental photolysis rate constant was also measured at noon and was assumed to decrease to zero in the night and increase from zero to the noon value. We assume that this rise and fall of the rate constant followed a sinusoidal distribution. We believe, however, that deviations from this assumption would produce an error no greater than a factor of two, based on our measurement of rate constants at noon and 4:00 P.M. in our laboratory.

We have assumed an average depth for the calculation of the environmental photolysis rate constant. We believe this is a reasonable approximation once TNT is distributed across the river. However, in the initial stage, the discharge is hugging the North Bank where the depth is much less than it is further into the river. This will tend to increase the phototransformation rate constant for that section of the river until average depth distribution is achieved.

In conclusion, this study demonstrates that models can be used to reliably predict RDX concentration in the aquatic environment, and that, therefore, they can be useful in hazard assessments. Insufficient data were obtained to make a similiar claim for TNT, due to low input concentration during the collection of field samples. However, from the data that were obtained, we conclude that the simulation model will approximate environmental TNT concentrations in the Holston River. This tends to make the use of pseudo-first-order rate expressions creditable for describing the loss and movement of aquatic pollutants and suggests that the laboratory determination of transformation rate constants can be usefully applied to aquatic systems.

The study also demonstrates the much greater complexity of a real aquatic system compared to our simulated model river and the need to incorporate more of the real-world complexity into the planning of field experiments and interpretation of the data. The great value of having a conservative chemical available with which to trace out the flow characteristics of the river is evident.

VI REFERENCES

Bordner, R., and J. Winter. 1979. Microbial Methods For Monitoring the Environment, Waters and Wastes. EPA Publication 600/8-78-017.

Buchanan, T. J., and W. P. Somers. 1969. Techniques of Water-Resources. Investigations of the United States Geological Survey, Chapter A8. Discharge Measurements at Gaging Stations, U.S. Government Printing Office, Washington, D.C. p. 1-4.

Guy, H. P., and V. W. Norman. 1970. Techniques of Water-Resources. Investigation of the United States Geological Survey, Chapter C2. Field Methods for Measurement of Fluvial Sediment, USGS, U.S. Government Printing Office, Washington, D.C. p. 5.

Mill, T., W. R. Mabey, D. C. Bomberger, T. W. Chou, and J. H. Smith. 1981. Laboratory Protocols for Evaluating the Fate of Organic Chemicals in Air and Water, draft report submitted in partial fulfillment of EPA Contract 68-03-2227. SRI International, Menlo Park, CA.

Smith, J. H., W. R. Mabey, N. Bohonos, B. R. Holt, S. S. Lee, T. W. Chou, D. C. Bomberger, and T. Mill. 1977. Environmental Pathways of Selected Chemicals in Freshwater Systems. Part II--Laboratory Studies. Final Report, EPA Contract 68-03-2227, SRI International, Menlo Park, CA.

Spanggord, R. J., T. Mill, T, W. Chou, W. R. Mabey, J. H. Smith, and S.Lee. 1980b. Environmental Fate Studies on Certain Munition Wastewater Constituents. Phase II--Laboratory Studies. Final Report, U.S. Army Medical Research and Development Command Contract, DAMD-17-78-C-8081, SRI International, Menlo Park, CA.

Sullivan, J. H. Jr., H. D. Putnam, M. A. Kiern, D. R. Swift, and B. C. Arnett, Jr. 1977. Aquatic Field Surveys at Holston Army Ammunition Plant, Kingsport, Tennessee. Final Report, Contract DAMD-17-75-C-5049, Water and Air Research, Inc., Gainesville, FL.

Zepp, R. G., and D. M. Cline. 1977. Rates of Direct Photolysis in Aquatic Environments. Environ. Sci. Technol. 11, 359-366.

DISTRIBUTION LIST

25 copies	Commander US Army Medical Bioengineering Research and Development Laboratory ATTN: SGRD-UBG Fort Detrick, Frederick, MD 21701
4 copies	Commander US Army Medical Research and Development Command ATTN: SGRD-RMS Fort Detrick, Frederick, MD 21701
12 copies	Defense Technical Information Center (DTIC) ATTN: DTIC-DDA Cameron Station Alexandria, VA 22314
1 copy	Dean School of Medicine Uniformed Services University of the Health Sciences 4301 Jones Bridge Road Bethesda, MD 20014
1 copy	Commandant Academy of Health Sciences, US Army ATTN: AHS-CDM Fort Sam Houston, TX 78234
1 copy	Commander US Army Medical Bioengineering Research and Development Laboratory ATTN: SGRD-UBD-A/Librarian Fort Detrick, Frederick, MD 21701